Gas source for fluidisation

Smith (1960a), Sparks (1976) and Wilson (1980) have identified the principal sources of gas for the fluidisation of pyroclastic flows. Wilson (1980) provided some criteria which could be used to assess the importance of internal gas sources (that is, residual magmatic volatiles released from juvenile pyroclasts) in comparison with external gas sources (such as, ingestion of air, steam generated from trapped groundwater or surface water, gas from combustion of vegetation). The former are mainly responsible for vertical textural variations in pyroclastic flow deposits, whereas the latter promote proximal-distal lateral zonation (Wilson, 1980).

Ingestion of air at the site of initial flow formation is correlated with a brief but very efficient fluidisation event that may result in segregation of co-ignimbrite lag breccias, proximal pyroclastic ground surge deposits and excessive crystal enrichment (Wilson, 1980; Wright and Walker, 1981; Wright, 1981; Druitt and Sparks, 1982). Entrapment of air at the front of a pyroclastic flow leads to the differentiation of a fluidised head from the rest of the body of the flow (Wilson, 1980). The two parts leave different deposits; for example, fines-depletion and enrichment in coarse and/or dense components, and also layering, are characteristic of flow head deposits (e.g. 'fines-depleted ignimbrite' of Walker, Wilson and Froggatt, 1980; 'ground layer' of Walker, Self and Froggatt, 1981; 'Layer 1' of Wilson and Walker, 1982; 'ground breccia' of Druitt and Sparks, 1982). Wright *et al.* (1984) have described Quaternary pumice- and ash-flow deposits of St Lucia, West Indies, marked by exceptional fines depletion. Gas from combustion of vegetation and turbulence caused by the nature of the flow paths probably significantly contributed to fluidisation during transport, in addition to flow-front air ingestion. It is thus possible to detect the effects of former fluidisation by flow front air ingestion, or other external sources of gas, in the resulting ignimbrite.

There is no sign that air ingestion, or any other external gas supply, either at source or enroute, influenced the emplacement of the Normal facies pyroclastic flows. The Normal facies ignimbrite is not known to be associated with lag breccias or ground breccias, lateral facies variation is negligible and there is no excessive crystal enrichment. That is, the ignimbrite is almost entirely composed of pyroclastic flow body deposits. The thin interval thought to have been deposited by pyroclastic ground surges is volumetrically minor (less than 0.1 km^3), areally restricted and confined to a single stratigraphic level, and is interpreted to register the initial flow formation by eruption column collapse (discussed further below).

It is clear that air ingestion was not an effective gas supply for fluidisation. However, there is little evidence that the alternative, an internal gas supply, was any more significant. Residual magmatic volatiles may produce gas flow rates sufficient to fluidise significant amounts of fine ash, especially in the upper parts of thick pyroclastic flows (Sparks, 1978a). The substantial thicknesses of Normal facies ignimbrite available are essentially texturally homogeneous, although admittedly the effects of gas grading can be very subtle (*cf.* Wright and Walker, 1981; Wright, 1981). Nevertheless, the poorly fluidised condition of the Normal facies pyroclastic flows attests to the inadequacy of residual magmatic volatiles as a source of gas for fluidisation.

Pyroclastic flow velocity and aspect ratio of the Normal facies ignimbrite

Wilson and Walker (1981,1982; Fig. 6) related the spectrum of pyroclastic flow types to flow velocity. Their analysis shows that air ingestion at the flow front is promoted by high flow velocity. Air ingestion fluidisation is insignificant or minor for flows travelling less than about 30 m/s. In view of the poor fluidisation inferred for the Normal facies pyroclastic flows, their velocities are unlikely to have exceeded a few tens of metres per second.

The aspect ratio of an ignimbrite is another means by which pyroclastic flow velocity can be qualitatively assessed (Walker *et al.*, 1980a,b; Wilson and Walker, 1981; Walker, 1983). The three dimensional geometry of deposits from high velocity pyroclastic flows is exemplified by low-aspect ratio ignimbrites. These are comparatively thin but widespread, show little evidence in their distribution of the flows having been topographically controlled, and exhibit mappable lateral variations in facies; aspect ratios of the Taupo (1:70,000; Walker *et al.*, 1980a; Wilson and Walker, 1981) and Rabaul (1:7000; Wilson and Walker, 1981; Walker, Heming *et al.*, 1981) ignimbrites are considered low (Walker, 1983). In comparison, the passage of low velocity pyroclastic flows shows sensitive response to topographic controls and resultant deposits form high-aspect ratio geometries. The Rio Caliente ignimbrite has a high aspect ratio (1:300; Wright, 1981).

Using an area (450 km^2) slightly larger than the present Coombadjha Volcanic Complex (360 km^2) as an estimate of the former extent of the Normal facies ignimbrite within the Coombadjha cauldron, and a value of 600 m for average thickness, gives an aspect ratio of 1:40 (Table 8.4). This is considered to be the lowest reasonable result, as the thickness is an underestimate. Even after doubling the area estimate (to 1000 km^2), the aspect ratio is reduced only slightly to 1:70. The Normal facies ignimbrite has an exceptionally high aspect ratio although comparable values would be expected for as yet unmeasured Tertiary intracaldera ignimbrites of the western United States. For example, the data of Ratté and Steven (1967, p.H42) indicate that the intracaldera Snowshoe Mountain Quartz Latite has an aspect ratio of 1:10 (Table 8.4). The lowest aspect ratio cited by Walker *et al.* (1980a) was 1:250 for the Bishop Tuff, California, and presumably includes the outflow sheets of this unit.

The high aspect ratio of the Normal facies ignimbrite is another hallmark of emplacement by slow-moving, relatively immobile pyroclastic flows. Flows with velocities of 30 m/s would be blocked and diverted by all obstacles higher than about 50 m (*cf.* Francis and Baker, 1977, Fig. 2) so that their deposits accumulate in high-aspect ratio bodies. Confinement within a caldera, or any other topographic depression, will contribute to, but not cause, the high aspect ratio of ignimbrites deposited by poorly fluidised, slow moving pyroclastic flows.

Style of eruption and emplacement of the Normal facies pyroclastic flows

The generation and movement of silicic pyroclastic flows are currently referred to a model involving the gravitational collapse of a vertical eruption column (Sparks and Wilson, 1976; Wilson, 1976; Sparks *et al.*, 1978; Wilson *et al.*, 1978,1980). To some extent the model allows reconstruction of the course of an eruption from the character and distribution of the deposits. It also permits evaluation of the conditions at the

TABLE 8.4: Dimensions and aspect ratios of the Dundee Rhyodacite of the Coombadjha Volcanic Complex, the Fish Canyon Tuff (Lipman, 1975; Steven and Lipman, 1976), the Snowshoe Mountain Quartz Latite (Ratté and Steven, 1967) and the Fish Creek Mountains Tuff (McKee, 1970)

	area (km^2)	thickness (m)	volume (km^3)	aspect ratio[1]
Dundee Rhyodacite, Coombadjha Volcanic Complex	450	600	270	1:40
	450	1000	450	1:24
Fish Canyon Tuff, Colorado intracaldera ignimbrite	1250	1400	1750	1:29
Snowshoe Mountain Quartz Latite, Colorado intracaldera ignimbrite	206	1600	330	1:10
Fish Creek Mountains Tuff, Nevada intracaldera? ignimbrite	515	610	315	1:42

[1]Aspect ratio calculation follows Walker *et al.* (1980a):

$$\text{Aspect ratio} = \frac{\text{average thickness}}{\text{diameter of circle with the same area}}$$

vent known to influence eruptive style (e.g. Wright, 1981). Using this approach, several lines of evidence suggest that the pyroclastic flows responsible for the Normal facies were produced by a continuously collapsing ignimbrite fountain fed by a low eruption column, which was established without any initial convective plume phase.

Nowhere beneath the Normal facies has a pumice- or ash-fall tuff potentially related to the ignimbrite been identified, suggesting that column collapse took place without an established convective plume phase (*cf.* Sparks *et al.*, 1973). Although prevailing wind directions during an eruption can distribute airfall deposits independently of related ignimbrite (e.g. Roseau pyroclastic flow deposits to the west, and plinian airfall tephra to the east, of the source on Dominica, Lesser Antilles; Carey and Sigurdsson, 1980), there is an independent, though indirect, argument in support of the conclusion that no convective phase was established. Sparks and Wilson (1976) demonstrated that most eruptions commencing with a convective plume produced ignimbrites with low emplacement temperatures. The Normal facies ignimbrite has welding and recrystallisation features indicative of high emplacement temperatures, consistent with the absence of an associated airfall deposit.

Sparks *et al.* (1978) calculated collapse heights of 600 m to 9 km above the vent and the ignimbrite fountains in the models of Wilson *et al.* (1980) were all less than 10 km high. Pyroclastic flows formed from the collapse of eruption columns at the high end of the predicted range are thought to undergo a vigorous fluidisation episode at the site of initial flow formation (Wilson, 1980) which is recorded by deposition of proximal co-ignimbrite lag breccias (e.g. Wright and Walker, 1981; Druitt and Sparks, 1982). Away from the source, such flows sustain high flow velocities and are effectively fluidised, especially by flow front air ingestion, so that ground breccias (Layer 1 of Wilson and Walker, 1982), marked textural variations, and excessive crystal enrichment are typical (Sparks *et al.*, 1978; Wilson, 1980; Wilson and Walker, 1981,1982; Wright, 1981). The pyroclasts are significantly cooled during column collapse so that subsequent welding of deposits is inhibited.

The Normal facies ignimbrite displays very little resemblance to pyroclastic flow deposits correlated with collapse from a high eruption column: no exposures of co-ignimbrite lag breccias have been found and the pyroclastic flows are inferred to have been poorly fluidised and slow moving. In addition, the ignimbrite was emplaced at temperatures high enough for thorough welding, devitrification and recrystallisation of formerly vitric pyroclasts. Comparison of vent radius and upward gas velocity estimates for the Dundee eruption (Table 8.5; discussed further below) with the models presented graphically by Sparks *et al.* (1978, Fig. 1, Fig. 3) suggests collapse heights may have been as low as 2 to 4 km, and are unlikely to have exceeded 6 km.

That the initial eruption column collapse was sustained to form an eruptive fountain is a conclusion based on the lithological homogeneity of the Normal facies ignimbrite. Above the base of the Normal facies, there are no changes which could be correlated with interruption to the discharge, or with alteration in its style. Further, there is only one lithological record of column collapse. The bedded tuff of the Basal facies is considered to include pyroclastic ground surge deposits. These occupy a stratigraphic position consistent with the interpretation that the surges were generated at the onset of column collapse which was thereafter maintained. Any pause significant enough to terminate the erupting fountain would be followed by another collapse event on reinstatement of activity. Bedded tuff, or other lithological variants to the Normal facies ignimbrite, would register such deviations. Sparks *et al.* (1973) suggest that breaks as brief as an hour would be sufficient for settling of co-ignimbrite ash (Layer 3) between flow units. Continuous production of pyroclastic flows is thus inferred.

Duration of the eruption of the Dundee Rhyodacite

Estimation of the duration of the Dundee Rhyodacite eruption episode is a poorly constrained procedure, especially without the guide of recorded events analogous in scale and style. The durations of large volume explosive eruptions have been deduced using measured subaqueous settling rates of associated airfall ash and other sophisticated techniques (e.g. Wilson and Walker, 1981; Wright, 1981). Ledbetter and Sparks (1979) estimated 20 to 27 days for a Quaternary eruption from Lake Atitlan caldera, Guatemala, which produced 250 km^3 (DREV) of rhyolitic ignimbrite and ash-fall tuff. The 1000 km³ Toba eruption, Sumatra (0.75 Ma) has been estimated to have lasted 9 to 14 days (Ninkovich *et al.*, 1978; Ledbetter and Sparks, 1979). Wright (1981) calculated 15 to 31 days for the Pleistocene eruption of 32.5 km³ (DREV) of ignimbrite and airfall deposits from Sierra La Primavera volcano, Mexico, the lithological record of which includes many signs of interruptions to discharge.

It is apparent from these examples that an eruption lasting at least a few weeks would be necessary for the emplacement of ignimbrites such as the Normal facies of the Dundee Rhyodacite in the Coombadjha Volcanic Complex. Accumulation of the Basal facies may have been much slower, as it is likely that significant quiescent spells separated eruptions of the ignimbrite and the lava (perhaps tens of thousands of years?; *cf.* Mahood, 1980; Hildreth, 1981).

Controls on the character and course of the eruption of the Normal facies ignimbrite

As interpreted above, the eruption of the Normal facies involved prompt collapse of a low eruption column and establishment of a sustained pyroclastic flow-forming fountain. Theoretical analyses of controls on the behaviour of explosive eruption columns have isolated those conditions which promote column collapse and the ensuing production of pyroclastic flows (e.g. Sparks and Wilson, 1976; Wilson, 1976; Sparks *et al.*, 1978; Wilson *et al.*, 1978,1980). In brief, these are:

i. large or increasing vent radius;
ii. relatively low or decreasing upward gas velocity;
iii. relatively low or decreasing magmatic gas content.

In addition, a high volume rate of eruption may also favour column collapse because this circumstance arises with widening vents and decreasing gas contents (Wilson *et al.*, 1978). Relatively coarse grained pyroclast populations in the eruption column will also be conducive to collapse because large particles are less efficient in contributing their heat to drive convection (Settle, 1978; Wilson *et al.*, 1978). All these factors influence the density of the eruption column at the top of the gas thrust region and determine whether progression to convective plume activity, or column collapse, ensues.

In the following discussion an attempt is made to assess the controls on the character and course of the eruption that produced the Normal facies.

Vent radius

The number and dimensions of vents for the Normal facies eruption are unknown. Crude estimates of vent radius ranging from about 350 m to 500 m were determined (Table 8.5), using the equations of Wilson (1976, Equations 18,19, p.554) which relate mass erupted and duration of plinian events. The calculations require an approximation of the upward gas velocity, although the value chosen has only a minor effect on the results (Table 8.5). Comparable estimates of vent radius are indicated by the models of Wilson *et al.* (1980, Figs. 7 and 9) for the mass eruption rate of the Normal facies event of about 10^8 kg/s (Table 8.6a). Vent radii adopted in theoretical models range from tens of metres to more than 600 m (e.g. Wilson *et al.*, 1978,1980; Sparks *et al.*, 1978), and it is concluded that the vent(s) for the Normal facies eruption episode had dimensions near the wide end of this range.

It can also be inferred that stable vent dimensions were achieved very soon after the onset of the Normal facies eruption. The proportion of lithics in the Normal facies ignimbrite is very low and they are only conspicuous in samples from near the base. The Basal facies ignimbrite has a relatively high proportion of dense lithics. If both facies had the same or nearby vents, the earlier Basal facies ignimbrite eruption may have achieved most of the necessary conduit excavation. There is a ubiquitous though minor component of millimetre sized gabbroic and dioritic crystal aggregates in the ignimbrites of both facies which may have significance with regard to magma chamber processes (cumulate disruption and roof or wall disintegration respectively), but are unlikely to reflect events affecting the conduit(s) and/or vent(s).

Wilson *et al.* (1980) examined the effects of conduit geometry on the eruption velocity of the gas-particle mixture. Conduits that had constant or decreasing radii near the surface were shown to retard eruption velocities, and to increase the gas pressure, and hence also the gas

TABLE 8.5: Estimates of vent radii for the Normal facies ignimbrite of the Dundee Rhyodacite, Coombadjha Volcanic Complex

vent radius[1], $b_o = \sqrt{\dfrac{m_t\ n}{q\ U_o\ \pi\ T_e\ 100\rho_o}}$ where $m_t \equiv$ total mass of pyroclasts;

n, U_o are average magma volatile content and muzzle velocity;

$T_e \equiv$ eruption duration;

$\rho_o \equiv$ initial gas density;

$q \equiv$ ratio of average upward velocity across eruption column to central value.

For $q = 1$, $\rho_o = 0.18$ kg/m³ for steam at 1200K, and average $U_o = 0.5\ U_o$ maximum,

$$b_o = \sqrt{\frac{m_t\ n}{9\ \pi\ T_e\ U_o}}$$

For the Normal facies ignimbrite of the Dundee Rhyodacite, assuming

$$m_t = 1.125 \times 10^{15}\ \text{kg}$$

$$T_e = 21\ \text{days}$$

$$= 1.8 \times 10^{6}\ \text{seconds}$$

$$b_o = \sqrt{\frac{2.21 \times 10^{7}\ n}{U_o}}\ .$$

n (weight %)	U_o (m/s)	b_o (m)
2	400	332
	300	384
	200	470
3	400	407
	300	470
4	300	542

[1]From Wilson (1976), equations (18) and (19).

density, in the vent for the range of magma volatile contents tested (up to 7 weight percent). Thus, the rapid formation of stable, probably wide and non-flared vent(s) may have placed limits on the upward gas velocity of the Normal facies eruption, a condition favourable to premature column collapse, inferred from stratigraphic evidence.

Upward gas velocity

The upward gas velocity at eruption controls (with vent radius) the collapse height of the eruption column (Sparks *et al.*, 1978). Because pyroclastic flows inherit significant momentum from the collapse event, especially those produced from vents within low profile rhyolitic calderas, the character of their deposits reflects the collapse height (Sparks, 1976; Francis and Baker, 1977; Sparks *et al.*, 1978; Sheridan, 1979; Wilson and Walker, 1981). The Normal facies pyroclastic flows are thought to have been slow moving, poorly fluidised and emplaced at high temperatures, matching the character of flows predicted to result from low collapse heights (Sparks *et al.*, 1978; Wilson and Walker, 1981). Upward gas velocities can thus be indirectly inferred to have been relatively low in this case, a conclusion consistent with the lithological record of premature column collapse. Eruption velocities up to 600 m/s are used in the theoretical models (e.g. Wilson *et al.*, 1978,1980; Sparks *et al.*, 1978). However, for non-flared conduits, vent eruption velocities are less than 200 m/s for magma water contents up to 7 weight percent (Wilson *et al.*, 1980, Fig. 8). Thus the proposed absence of flaring in the Normal facies ignimbrite vent(s) is consistent with relatively low upward gas velocity during eruption. Velocities were probably in the lower half of the theoretically considered range.

Released gas content

Magmas with high water content have the potential to release large amounts of gas (largely steam) when erupted and are capable of sustaining convective plume activity, whereas those eruptions involving low released gas content require excessively high gas velocities or very narrow vents in order to avoid column collapse (Wilson, 1976; Sparks *et al.*, 1978). Gas content has a relatively minor effect on the height at which column collapse occurs, though collapse height increases with larger gas contents (Sparks *et al.*, 1978).

There is no direct means for establishing the pre-eruption dissolved volatile content of the Dundee Rhyodacite magma. However, there are no positive indications that it had the potential to release large gas contents during eruption and indirect arguments suggest the converse. The eruption of the Normal facies ignimbrite was preceded by extrusion of phenocryst-rich lava, an event interpreted as an early sign of the low volatile content of the magma supply because the production of pyroclastic flows more commonly follows a gas-rich plinian stage (Sparks *et al.*, 1973; Sheridan, 1979; Hildreth, 1981). At eruption, the Dundee Rhyodacite magma was similarly phenocryst-rich (at least 45 weight percent), including about 10 weight percent hydrous minerals (biotite and hornblende).

The character of the Normal facies pyroclastic flows and the ignimbrite they deposited is consistent with two implications of low released volatile content. Firstly, it has been inferred above that the main gas source for fluidisation of the Normal facies pyroclastic flows was internal, that is, dependent on the volatile contents of juvenile pyroclasts. This supply is potentially adequate for efficient fluidisation (Sparks, 1978a) but was clearly incapable of effectively fluidising the Normal facies pyroclastic flows beyond the condition typical of type 1. Secondly, the Dundee Rhyodacite ignimbrite was originally welded and vitric pyroclasts are completely devitrified and substantially recrystallised. There are two ways in which low released gas content promotes a high temperature of emplacement of pyroclastic flows:

i. this circumstance is consistent with low column collapse height, predicted to enhance heat conservation by inhibiting entrainment of air (Sparks and Wilson, 1976; Sparks *et al.*, 1978);

ii. the smaller proportion of hot pyroclasts in gas-rich columns fed by magmas releasing several weight percent gas during eruption reduces their conservation of heat relative to columns involving lower released gas content (Sparks *et al.*, 1978).

These stratigraphic and lithological clues are the basis for interpreting comparatively low released gas content for the Dundee Rhyodacite eruption episode, a conclusion in accord with the record of early enstatement of a pyroclastic flow-forming eruption fountain without prior establishment of a plinian phase.

Discharge rate

For an eruption duration of 3 weeks, the mass eruption rate for the Normal facies ignimbrite is approximately 6 x 10^8 kg/s and volume eruption rate is 25 x $10^5 m^3/s$ (Table 8.6a). Both these figures are near the maxima of rates considered in the theoretical models of Wilson *et al.* (1978, 1980) though comparable to data from other large volume silicic ignimbrite eruptions (Table 8.6b). Wilson *et al.* (1978, p.1835) predicted that volume eruption rates in excess of 6.5 x $10^5 m^3/s$ would lead to eruption column collapse. The high discharge rate for the Normal facies ignimbrite eruption is consistent with two previous and related conclusions: that wide vents were involved, and that conditions were never appropriate for transformation of the gas thrust of the eruption into a maintained convecting plume. Instead, the eruption column is thought to have very promptly collapsed downward.

Degree of magma fragmentation

Progression of explosive eruptions from the initial gas thrust to a maintained convecting plume requires efficient transfer of the magmatic heat of the pyroclasts to entrained air (Wilson, 1976; Settle, 1978; Wilson *et al.*, 1978). The efficiency of exchange depends on the grain size of pyroclasts and the theoretical models assume that 60 weight percent or more of pyroclasts are less than a millimetre in diameter (Sparks and Wilson, 1976; Wilson, 1976; Sparks *et al.*, 1978; Wilson *et al.*, 1978; Wilson *et al.*, 1980). At the time of vesiculation and eruption, the Dundee Rhyodacite magma was at least 45 weight percent crystals or crystal aggregates generally coarser than 1 mm. The implication of a relatively coarse pyroclast population which was already substantially crystalline is that the heat needed to drive plume convection may not have been available from the outset. The conservation, rather than transfer, of the heat energy of the pyroclasts may have contributed to premature column collapse.

Summary

The eruption of the Normal facies ignimbrite, as reconstructed here, involved from the outset a pyroclastic flow-forming fountain of moderate to low height. The stratigraphy and lithological character of the Normal facies ignimbrite provide indirect evidence that the eruption was marked by low upward gas velocity, low released gas content, very high discharge rate and a comparatively coarse pyroclast population. These conditions, in conjunction with large vent radii, are predicted by theoretical models to be necessary for the envisaged eruption behaviour (Sparks and Wilson, 1976; Wilson, 1976; Sparks *et al.*, 1978; Wilson *et al.*, 1978,1980). No aspects of the geology of the Normal facies are incompatible with the additional inference of non-flaring, probably wide vent(s).

The "bigness" of the Normal facies eruption episode

The parameters used to measure the "bigness" of explosive eruptions, reviewed and further refined by Walker (1980,1981e), are here applied to the Normal facies eruption episode.

Magnitude measures the dense rock equivalent volume erupted and the scale ranges from 0.001 km^3 to 1000 km^3. The volume of the Normal facies of the Dundee Rhyodacite is presently more than 200 km^3 and originally may have been as much as 450 km^3 (Table 8.6a). It was densely welded on emplacement so these figures are effectively dense rock equivalent volumes. Hence, the order of magnitude of the entire volume erupted, including probable outflow sheets and co-ignimbrite ash, may have approached 1000 km^3, and was clearly of enormous magnitude. The Normal facies ignimbrite has magnitude 2 on Smith's (1979) scale of ash flow eruptions, and has the same order as some Tertiary intracaldera ignimbrites (e.g. 330 km^3, Snowshoe Mountain Quartz Latite, Ratté and Steven, 1967) but is much less than the most voluminous examples (e.g. about 1200 to 1800 km^3 for the intracaldera part of the Fish Canyon Tuff, Colorado; Lipman, 1975; Steven and Lipman, 1976).

Intensity is the term used for the rate of release of material, in dense rock equivalent volume, or of energy (Walker, 1980). The volume eruption rate for the Normal facies ignimbrite was approximately 6×10^5 m^3/s (Table 8.6a), corresponding to the class of high intensity eruptions (between 10^3 and 10^6 m^3/s, Walker, 1980). The duration would have to have been 10 times longer than estimated to achieve a reduction in the order of the volume eruption rate, but would not shift the event from the class of high intensity eruptions.

Violence reflects the importance of momentum in the emplacement and distribution of the products of an explosive eruption (Walker, 1980,1981e; Wilson and Walker, 1981). The violence of eruptions producing pyroclastic flows is expressed by flow velocity and the morphology of their deposits. The Normal facies pyroclastic flows had a low velocity and the preserved deposits suggest they built a high-aspect ratio ignimbrite pile.

Although the eruption of the Normal facies ignimbrite was outstanding in magnitude and intensity, it was an event unspectacular in violence.

Cessation of eruption

The Dundee Rhyodacite eruption episode can only be reconstructed for the existing incomplete lithological record so the course of the later stages is unknown. The history of events leading to the formation of the Coombadjha cauldron are thought to indicate that major subsidence did not begin until after the emplacement of most of the preserved thickness of the Normal facies ignimbrite (Chapter 6). If the eruption duration is taken as a measure of the time involved in evacuation of the Dundee Rhyodacite magma supply, it is perhaps not unreasonable to find that there was a delay before movements on the ring fracture system and cauldron subsidence began. Later eruptions, inferred on the basis of the total amount of collapse, may have been accompanied by sagging of the cauldron floor and displacement along incipient ring fractures. A major subsidence event at a stage when activity was waning could ultimately have been responsible for terminating discharge from ring fault-located vents (*cf.* Wilson *et al.*, 1980).

Post-emplacement modification and preservation of the Normal facies ignimbrite

The thorough welding, devitrification and recrystallisation exhibited by formerly glassy pumiceous components of the Normal facies ignimbrite throughout the Coombadjha Volcanic Complex are largely attributable to the large magnitude and low violence of the eruption. These parameters together determined the character of the Normal facies pyroclastic flows,

TABLE 8.6a: Measures of "bigness" of the eruption of the Normal facies of the Dundee Rhyodacite, Coombadjha Volcanic Complex

MAGNITUDE:		
dense rock equivalent volume	450 km^3	large
	4.5×10^{11} m^3	
mass	1.125×10^{15} kg	
INTENSITY:		
volume eruption rate (21 days)	2.5×10^{5} m^3/s	high
mass eruption rate (21 days)	6×10^{8} kg/s	
VIOLENCE:		low

TABLE 8.6b: Intensities of the Normal facies ignimbrite eruption and other ignimbrite-producing eruptions

	volume eruption rate (m^3/s)	DRE volume (km^3)
Dundee Rhyodacite: Normal facies ignimbrite	2.5×10^{5}	450
Toba[1], Indonesia: ignimbrite and airfall ash	10^{6}	1000
Los Chocoyos[2], Guatemala: ignimbrite and airfall ash	2.4×10^{5}	250
Rio Caliente Ignimbrite[3], Mexico: ignimbrite and co-ignimbrite ash	1.4×10^{4}	18.5
Taupo Ignimbrite, New Zealand[4]: ignimbrite and co-ignimbrite ash	3×10^{7}	12
Valley of Ten Thousand and Smokes[5], Alaska: ignimbrite	2×10^{5}	5.5

[1]Ninkovich, Sparks and Ledbetter (1978).

[2]Ledbetter and Sparks (1979).

[3]Wright (1981).

[4]Wilson and Walker (1981).

[5]Curtis (1968).

and ensured their emplacement at high temperatures and the pronounced compaction of their deposits. The Normal facies ignimbrite probably had a low initial porosity which may have been important in inhibiting alteration of crystal fragments; these are noticeably fresher than crystal fragments and phenocrysts of most of the other volcanic units of the Coombadjha Volcanic Complex.

All surviving exposures of the Normal facies ignimbrite are erosional remnants of a thicker simple (or compound) cooling unit, the preservation of which is due to subsidence of the Coombadjha cauldron.

SIMILAR CAINOZOIC IGNIMBRITES

Although the Dundee Rhyodacite of the Coombadjha Volcanic Complex is a remarkable rock unit, it is by no means unique. The following brief descriptions of three Tertiary ignimbrites of the western United States support this conclusion. All three have comparable composition (high K_2O dacites), lithology (crystal-rich, texturally homogeneous ignimbrite) and volume (hundreds of cubic kilometres) to the Dundee Rhyodacite.

The La Jara Canyon Member

Eruption of the La Jara Canyon Member of the Treasure Mountain Tuff (29.8 Ma) led to subsidence of the Platoro caldera (Lipman, 1975; Steven and Lipman, 1976). Vent locations are unknown. About half (250 km^3) of the total volume of ignimbrite of this Member (580 km^3) is within the caldera where it is more than 800 m thick at some localities. The aspect ratio of the densely welded, crystal-rich (40 to 50 modal percent crystals) intracaldera ignimbrite is approximately 1:40. Lipman (1975) reported that it is largely devitrified and pumice fragments and flow unit boundaries are both masked by post-emplacement changes. Although there are no intercalations of "landslide breccias" in the intracaldera ignimbrite indicative of an exposed caldera wall, the late stages of the eruption were considered to have been accompanied by subsidence (Lipman, 1975). Evidently the first pyroclastic flows to be erupted spread widely as outflow sheets whereas subsequently, eruptions were concurrent with collapse (Steven and Lipman, 1976).

The Fish Canyon Tuff

The Fish Canyon Tuff, erupted from La Garita caldera, Colorado at 28.6 Ma (Lipman, 1975; Steven and Lipman, 1976; Whitney and Stormer, 1983) is lithologically similar to, but has a greater extent (15,000 km^2) and volume (3000 km^3) than what remains of the Dundee Rhyodacite in the Coombadjha Volcanic Complex. Outflow sheets of the Fish Canyon Tuff spread widely and ponded to exceptional thicknesses in all nearby topographic depressions including unrelated calderas (e.g. it is 1 km thick in the Mt Hope caldera; Steven and Lipman, 1976). The intracaldera ignimbrite has an aspect ratio of about 1:29, and although crystal-rich (approximately 53 weight percent crystals) the loss of vitric pyroclasts appears to have been very minor as the enrichment factor is only 1.2 (Table 8.3). Contrasts between the thickness of the outflow and intracaldera ignimbrite are interpreted to indicate concurrent cauldron subsidence and eruptions (Lipman, 1975; Steven and Lipman, 1976). The earliest inception of subsidence cannot be resolved because relationships at the base of the intracaldera ignimbrite are not exposed.

The Snowshoe Mountain Quartz Latite

Perhaps the best Cainozoic analogue for the Dundee Rhyodacite of the Coombadjha Volcanic Complex is the Snowshoe Mountain Quartz Latite (26.5 Ma) of Creede caldera, Colorado (Ratté and Steven, 1967; Steven and Lipman, 1976). Most of this unit is very thick (about 1.6 km) intracaldera ignimbrite with a volume of 330 km^3 and an aspect ratio of 1:10. It is densely welded and completely devitrified with vaguely defined pumice lapilli, and minor cooling and flow unit partings. Crystal fragments constitute about 55 weight percent of the ignimbrite although the enrichment factor is only 1.6 (Table 8.3). No vents have been located but are inferred to have been situated along part of the ring fracture zone (Ratté and Steven, 1967). Subsidence concurrent with ignimbrite eruption has been proposed (Ratté and Steven, 1967; Steven and Lipman, 1976). However "avalanche breccia" tongues are only known within the upper 700 m of the unit (Steven and Lipman, 1976, p.28), possibly indicating that collapse post-dated emplacement of a substantial thickness of ignimbrite. Because the base of the unit is not exposed in the caldera, the timing of initial subsidence is not known with precision.

Discussion

These examples are cited in order to illustrate that ignimbrites similar to the Dundee Rhyodacite of the Coombadjha Volcanic Complex are common as intracaldera fill although there are differences in their temporal and spatial relationships to host calderas. All are members of the "monotonous intermediates" magmatic group identified by Hildreth (1981). Such ignimbrites display minimal compositional variations throughout enormous volumes and are not apparently associated with more siliceous differentiates (Hildreth, 1981). Volcanological parallels cannot be demonstrated here but are by no means inconceivable. These voluminous densely welded, high-aspect ratio ignimbrites may also be the deposits of poorly fluidised pyroclastic flows generated by eruptions of large magnitude but relatively low violence.

REGIONAL IMPLICATIONS

The lithological uniformity of the widespread occurrences of crystal-rich ignimbrite (the Dundee Rhyodacite) of the Late Permian volcanic pile of New England is striking (Tables 8.1,8.2; Wilkinson *et al.*, 1964). However the original continuity of these areas of Dundee Rhyodacite ignimbrite is an unlikely circumstance in view of some of the conclusions reached with regard to the representative occurrence in the Coombadjha Volcanic Complex (*cf.* Flood *et al.*, 1977, p.301). Specifically, the crystal-rich ignimbrite of the Coombadjha Volcanic Complex was generated by an eruption of large magnitude but low violence, resulting in deposits with exceptional thickness and limited lateral extent. If the same style of eruption and emplacement proves applicable to the occurrences of crystal-rich ignimbrite elsewhere, they were probably originally discrete bodies, as at present. Furthermore, it is apparent from descriptions (Wilkinson *et al.*, 1964; Flood *et al.*, 1977; Cuddy, 1978; Wood, 1982) and reconnaissance inspection of the Dundee Rhyodacite of other areas that each of these is part of a densely welded, thoroughly recrystallised, incomplete (that is, eroded) cooling unit lacking in the typical features of outflow sheets and locally very thick (e.g. 1.5 km at Dundee, Shaw *et al.*, 1982). In contrast, the outflow sheets produced by major Cainozoic caldera-forming ignimbrite eruptions, such as the Fish Canyon Tuff, Colorado, are texturally distinguishable from essentially coeval intracaldera fill (J.V. Wright, written comm., 1984) even where ponded to exceptional thicknesses and densely welded.

The Dundee Rhyodacite had an intracaldera setting at Coombadjha (and Timbarra), and probably also at Dundee (Flood *et al.*, 1977; Godden, 1982; Shaw *et al.*, 1982). Resolution of the status of the remaining occurrences at Bolivia, Brassington, Tenterfield and Tarban must await further field studies. It is tentatively concluded that very little of the ignimbrite can be attributed to a formerly co-extensive outflow sheet. An alternative is suggested by the former proximity of the Tenterfield, Coombadjha and Brassington areas of the Dundee Rhyodacite prior to movement on the Demon Fault System (Appendix A). In plan, the arrangement is similar to Cainozoic nested cauldrons of the western United States (e.g. Yellowstone caldera complex, Wyoming, Eaton *et al.*, 1975; Christiansen, 1979; Timber Mountain-Oasis Valley caldera complex, Nevada, Byers *et al.*, 1976; clustered calderas of the western and central San Juan Volcanic Field, Colorado, Steven and Lipman, 1976). Formation of the adjacent Uncompahgre and San Juan calderas was essentially simultaneous and each is filled by the same intracaldera ignimbrite unit (Eureka Member; Steven and Lipman, 1976).

CONCLUSIONS

The Normal facies of the Late Permian Dundee Rhyodacite of the Coombadjha Volcanic Complex constitutes the lower 500 m of an originally thicker, densely welded, in places recrystallised, simple (or compound) cooling unit of crystal-rich ignimbrite. This ignimbrite has a very high aspect ratio and was deposited from poorly fluidised, weakly expanded, low velocity, type 1 (Wilson, 1980) pyroclastic flows which were sensitive to topographic control. Losses of fine grained pyroclasts were not extreme and probably took place at the site of eruption because elutriation from flows of this type can only have been minor.

The emplacement of thick, texturally uniform, crystal-rich ignimbrite was preceded by discharge of small volumes of compositionally similar, crystal-rich lava and ignimbrite. Thereafter the eruption episode was continuous and involved a sustained pyroclastic-flow forming fountain of low to moderate height. There was a delay before cauldron subsidence began at Coombadjha, although at later stages in the eruption, subsidence and ignimbrite production may have been concurrent.

Although of large magnitude (10^2 km^3) and probably high intensity (10^5 m^3/s), the eruption was of subdued violence. In particular, the combination of large magnitude and low violence appears to have been significant in determining the style of eruption and hence the character of the resulting pyroclastic flows and their deposits. No modern analogues for the Dundee Rhyodacite ignimbrite are known, but there are lithologically similar crystal-rich Cainozoic ignimbrites of comparable magnitude and in intracaldera settings.

Crystal rich ignimbrites are evidently uncommon in the Tertiary volcanic fields of the western United States (Smith, 1979). Smith (1979) interpreted this circumstance to be a reflection of the "maximum viscosity barrier" operating in the source magmas. That is, 40 to 50 percent crystals in magmas could be a limiting condition for their capacity to produce an ignimbrite eruption (Smith, 1979). The Dundee Rhyodacite magma was certainly close to this limit when erupted. Although silicic magmas which are substantially crystallised in many cases erupt to form atypical, high-aspect ratio ignimbrites exemplified by the Dundee Rhyodacite, they also supply eruptions that generate low-aspect ratio outflow sheets. Thus, it would seem that eruption style cannot be predicted solely on the basis of the properties of the porphyritic magma.

The causes of the character of the Normal facies ignimbrite of the Dundee Rhyodacite in the Coombadjha Volcanic Complex prevailed from the outset of its emplacement, when there was no caldera in existence at Coombadjha (Chapter 6). Although an intracaldera emplacement setting is a likely coincidence for voluminous, high-aspect ratio ignimbrites, the setting alone does not fully account for the contrasts these ignimbrites show with typical outflow sheets. This is also evident from cases where outflow ignimbrite is found ponded in unrelated calderas and yet remains distinguishable from the genuine, characteristically texturally homogeneous, high -aspect ratio intracaldera ignimbrites. Again, the eruption style is implicated as the primary determinant of the character of the Normal facies ignimbrite although style may have been influenced by processes attendant on cauldron formation, and by special properties of the crystal-rich magma, in a manner which is as yet unclear.

CHAPTER 9

SYNTHESIS AND SUMMARY

The first part of this synthesis attempts to integrate some of the separate threads of the foregoing chapters by focussing on the causes of facies diversity in the products of volcanic activity which was generally silicic in character and continental in setting. The discussion deals in turn with the control exerted by the circumstances of eruption (setting, style, magnitude), and the influence of proximity of sites of emplacement to the eruptive sources.

The second part summarises the main conclusions regarding the palaeogeographic setting of late Palaeozoic silicic volcanism in the southern portion of the New England Orogen.

VOLCANOLOGY

CIRCUMSTANCES OF ERUPTION

The role of external water

Ignimbrite members of the Currabubula Formation provide a clear illustration of contrasts in facies as functions of the involvement of external water. All the members were produced by explosive rhyolitic eruptions of similar magnitude (about 100 km^3 in volume) and were emplaced in much the same environment (braidplain). With one exception, the ignimbrite members display the 'normal' patterns of flow unit stratigraphy, systematic welding zonation and lateral and vertical changes in texture (*cf.* Smith, 1960a,b; Ross and Smith, 1961; Sparks *et al.*, 1973). The exception is the Cana Creek Tuff. The departure of this Member from the norm can be fully and effectively accounted for by the inference that external water was involved in its eruption and emplacement. Several features attest to the hydrovolcanic origin of the Cana Creek Tuff.

i. This member comprises a close association of primary pyroclastic facies (ignimbrite and ash-fall tuff) and compositionally equivalent, redeposited volcaniclastic facies (crystal-rich sandstone, pumiceous conglomerate).

ii. The ignimbrite of the pyroclastic facies is uniformly low-grade and relatively fine in grain size.

iii. Accretionary lapilli are present in the ignimbrite and in fine grained ash-fall tuff of the pyroclastic facies.

iv. The member is widely distributed and the internal arrangement of primary pyroclastic and redeposited volcaniclastic facies is complex.

v. Flood and debris flow deposits predominate in the volcaniclastic facies.

The Cana Creek Tuff shows vertical and lateral variations in proportions of primary and redeposited facies which may have been controlled by fluctuations in the water:magma mass ratio at the vent during the eruption, and by increases in condensation of steam with distance from the source.

Eruption style, mobility of pyroclastic flows and aspect ratio of ignimbrites

In reviewing studies of Cainozoic ignimbrites, Wilson and Walker (1981) demonstrated the importance of the style of an explosive eruption (especially its violence) in controlling the behaviour of the pyroclastic flows generated and hence also the nature of their deposits. A Palaeozoic illustration of this relationship has been inferred by comparing the character and distribution of the outflow ignimbrite sheets of the Currabubula Formation with the Dundee Rhyodacite of the Coombadjha Volcanic Complex. Each of the ignimbrite members of the Currabubula Formation is essentially similar in volume (100 km^3) and composition (high K_2O, silicic, calc-alkaline) to the Dundee Rhyodacite.

The ignimbrites of the Currabubula Formation are considered to be the deposits from adequately fluidised pyroclastic flows that had moderate to high velocities inherited from collapse of a vertical eruption column. Supporting evidence is as follows:

i. The ignimbrites have sheet-like geometry with low to moderate aspect ratios.

ii. Lateral and vertical variations in grain size are well developed and systematic, and flow units are in general clearly defined.

iii. Both welded and non-welded ignimbrites are present, as well as a number of instances of regular welding zonation within a single member.

This style of eruption is also responsible for additional features either not recognised or not established in the Currabubula Formation, such as enrichment of crystals in the ignimbrite relative to magmatic proportions, and the presence of a pumice- or ash-fall layer beneath the ignimbrite that records a prior stage of the same eruption.

The mobility of pyroclastic flows so formed commonly results in emplacement at sites at least several kilometres from the source in settings which are not affected by any collapse events accompanying eruption. By contrast, the Dundee Rhyodacite of the Coombadjha Volcanic Complex was deposited by slow-moving, poorly fluidised, topographically controlled pyroclastic flows generated by sustained collapse of an eruption fountain of comparatively low height. Such an origin is in accord with:

i. the high aspect ratio of the ignimbrite;

ii. lateral and vertical textural homogeneity of the ignimbrite;

iii. uniformly dense welding and pervasive recrystallisation of formerly glassy pumiceous components of the ignimbrite;

iv. slight enrichment of crystal fragments in the ignimbrite over magmatic proportions, as indicated by relic pumice;

v. the absence of a precursor pumice- or ash-fall layer beneath the ignimbrite;

vi. confinement of the ignimbrite to the vicinity of the eruptive source, the subsidence of which may have restricted flow mobility and contributed to the high aspect ratio.

The influence of magnitude and magma composition on hydrovolcanic facies

The two instances of Palaeozoic hydrovolcanism had disparate eruption magnitudes and they also differed slightly in composition. The Cana Creek Tuff involved a large magnitude rhyolitic hydrovolcanic eruption whereas the volcaniclastic facies of the Hianana Volcanics (Coombadjha Volcanic Complex) is the product of a small magnitude event of dacitic composition. The former generated an extensive sheet of ignimbrite, ash-fall tuff and redeposited volcaniclastic facies in which lateral variations are gradual over distances of several to tens of kilometres. The latter built a tuff ring of well-bedded surge facies closely confined to the vicinity of the vent, encircled by more widespread though thin airfall ash.

Vesiculated pumiceous pyroclasts are minor in the dacitic Hianana tuff ring deposits, but are the dominant component of the rhyolitic Cana Creek Tuff. It is inferred that vesiculation prior to magma-water interaction had reached a more advanced stage for the Cana Creek Tuff eruption than for the Hianana episode, and may be a reflection of the differences in magma compositions, especially SiO_2 and volatile contents, involved in each case (*cf.* Sparks, 1978b).

Lava-dominated ignimbrite centres and cauldrons

The Boggabri Volcanics and Coombadjha cauldron preserve the most proximal environments related to ignimbrite centres encountered in the course of this study. The Boggabri Volcanics are composed of large volumes of silicic lava and display no evidence of any collapse structure associated with the eruption of ignimbrites. Thus the Boggabri Volcanics exemplify an ignimbrite centre with constructional relief imparted by the lava pile that caps the pyroclastic apron, similar to the clusters of lava domes marking some of the ignimbrite centres of the Andes (e.g. Cerro Panizos, Baker, 1981).

Identification of the Coombadjha cauldron as an ignimbrite eruptive centre is based on the presence of thick, high-aspect ratio ignimbrite within a genetically related, large-scale subsidence structure that is encircled by a ring pluton. The Coombadjha cauldron is dissimilar in constitution and structure to the Boggabri ignimbrite centre, perhaps as a result of differences in the relative importance of effusive as against explosive eruption styles, and in the magnitude of eruptions in relation to the supply of magma.

PROXIMITY TO SOURCE

The Currabubula Formation and the Coombadjha Volcanic Complex each record the activity of ignimbrite-dominated silicic volcanic centres. Given that the style, scale and composition were comparable, the contrasts between these two sequences demonstrate the importance of proximity to eruptive centres as a control on the preserved lithofacies.

Medial to distal settings (more than several kilometres from the source volcanic centres), represented by the Currabubula Formation, display the following characteristics:

i. Primary volcanic units are principally outflow ignimbrites with overall sheet-like geometries.

ii. Ignimbrite sheets are separated by epiclastic facies (e.g. braidplain conglomerate in the Currabubula Formation). The proportion of epiclastic facies relative to ignimbrites increases with distance from eruptive sources.

iii. Because erosion is active at the depositional site, the stratigraphic record is biased in favour of voluminous and welded ignimbrites.

iv. The potential for overlap of ignimbrites produced at approximately the same time from nearby volcanic centres is low and diminishes with increasing distances from source.

In addition, the ignimbrites lack proximal facies indicators (e.g. co-ignimbrite breccias, coarse grained ground layers, lithic clasts larger than lapilli). Vent-produced pyroclastic surge deposits are absent, as are lavas and welded airfall tuffs. The ignimbrite-conglomerate stack accumulated beyond the influence of any collapse or intrusive events marking the eruption site.

The volcanic units emplaced in the Coombadjha area prior to formation of the Coombadjha cauldron constitute a proximal (extra-caldera) volcanic pile. Important identifying features are listed below.

i. Primary volcanic units are diverse. In addition to ignimbrites, lavas, block and ash flow deposits and pyroclastic surge deposits are present.

ii. The proportion of epiclastic and reworked pyroclastic facies is minor. Volcaniclastic deposits are principally breccias related to the ignimbrites or to the lavas and are of local or irregular extent.

iii. Ignimbrites may display pronounced changes in thickness over short distances reflecting the constructional relief of the site of emplacement.

iv. The stratigraphic pile incorporates ignimbrites from different volcanic centres because there is no filtering of the smaller volume or less extensive ignimbrites from the record.

v. Small-scale subsidiary volcanic centres are present (e.g. Hianana tuff ring, Babepercy lava dome).

PALAEOGEOGRAPHY

The regional setting of the Late Carboniferous explosive rhyolitic volcanism was that of a continental margin volcanic arc lining the edge of the Lachlan Fold Belt and accompanied to the east by a subaerial arc flank and submarine subduction complex (Leitch, 1975; Day *et al.*, 1978; Fergusson, 1982,1984a). The arc flank record (Currabubula Formation and equivalents) spans some 30 Ma of volcanogenic, braidplain gravel sedimentation interrupted by emplacement of ignimbrite sheets and glacial advances. Using an analogous section of the modern Andean arc as a guide, the Late Carboniferous volcanic terrain was most probably composed of stratovolcano mountains and ignimbrite centres (calderas and shields), the highest parts of which were intermittently clad by glaciers. The interplay between contemporaneous volcanic activity, glaciation and uplift of the volcanic terrain is inferred to have controlled the lithofacies constitution of the Late Carboniferous arc flank sequence, and produced the large and small scale disconformities within it. The compositions of the Late Carboniferous ignimbrites (high K_2O calc-alkaline rhyolites) are compatible with their sources having been within thick continental crust.

A similar tectonic and palaeogeographic configuration persisted into the Early Permian, at least for the limited section of the New England Orogen studied. Successions traditionally regarded as Late Carboniferous (*Rhacopteris*-bearing, e.g. the Currabubula Formation) and Early Permian (*Glossopteris*-bearing, e.g. the Temi Formation) have essentially conformable relationships and comprise generally similar lithofacies. Explosive volcanism continued but was accompanied by effusion of silicic lavas in proximity to the eruptive centres (e.g. at Boggabri) prior to final extinction of activity later in the Early Permian.

The cessation of major silicic volcanism from the Early Permian to the Late Permian in the southern part of the New England Orogen coincides with an interval during which the convergent, subduction-related tectonic configuration altered to a dextral, transcurrent regime involving the eastern edge of the entire Orogen (Murray and Whitaker, 1982). The older subduction complex of the southern part of the Orogen was deformed into a megafold and former deep marine environments were supplanted by shallow marine and continental settings. The latter prevailed at the resumption of widespread silicic volcanic activity in the Late Permian (Flood and Fergusson, 1982,1984).

The tectonic significance of the Late Permian silicic magmatism is uncertain and cannot be resolved solely on the basis of the character of the volcanic sequence. Such ignimbrite-dominated, high K_2O, silicic, calc-alkaline volcanism indicates little else than the presence of thick continental crust. Other workers have suggested that the Late Permian igneous activity represents the culmination of regional orogenesis essentially related to (but post-dating) the prior subduction-controlled regime (Leitch, 1975; Crook, 1980a), a response to circumstances operating in an entirely new transcurrent configuration (Flood and Fergusson, 1984), or the inception of subduction and convergence at a more easterly site (Shaw and Flood, 1981).

Though subordinate, basic igneous rocks are a typical accompaniment to the high-SiO_2, rhyolitic ignimbrites of extensional settings within continents (e.g. the western United States during the late Cainozoic; Christiansen and Lipman, 1972; Elston and Bornhorst, 1979; Hildreth, 1981), and andesitic volcanic rocks appear to be a characteristic component of magmatic arcs related to subduction (Coulon and Thorpe, 1981; Ewart, 1982; e.g. present day Andes, Thorpe *et al.*, 1982). As presently known, the Late Permian volcanics of New England do not closely match either of these settings because basalts are absent and andesitic extrusives are uncommon.

On a more local scale, it can be argued that the Coombadjha Volcanic Complex occupied an extensional setting : it is located on the limb of the megafold, offset by dextral movement on the Demon Fault and elliptical in plan, with the major axis parallel to the direction of extension implied by both the older megafold and the younger strike-slip fault (Fig. 9.1).

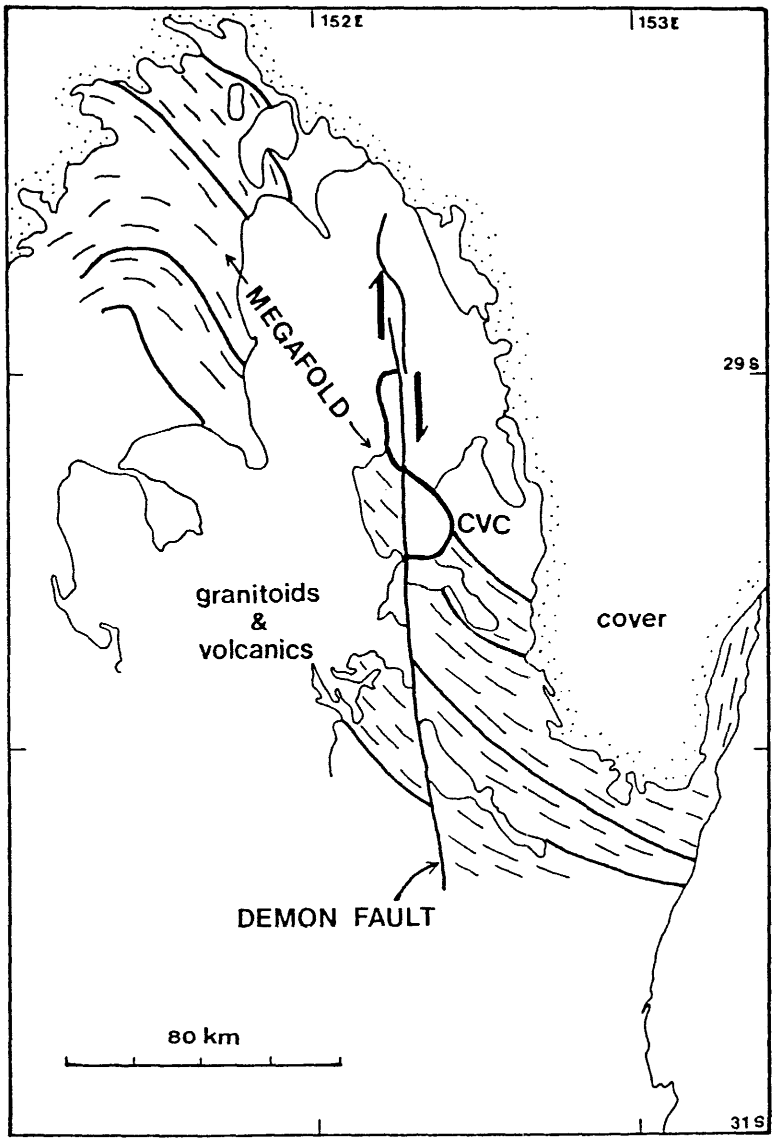

Figure 9.1: Schematic illustration of the setting of the Coombadjha Volcanic Complex in relation to the adjacent major structures, the Texas-Coffs Harbour megafold (Flood and Fergusson, 1982) and the Demon Fault System.

REFERENCES

Andrews, E.C. 1905. The geology of the New England plateau with special reference to the granites of northern New England, Parts II and III. Records Geol. Surv. N.S.W. 8:108-152.

Andrews, E.C., Mingaye, J.C.H. and Card, G.W. 1907. The geology of the New England plateau, with special reference to the granites of northern New England, Part IV. Records Geol. Surv. N.S.W. 8: 196-238.

Archbold, N.W. 1982. Correlation of the Early Permian faunas of Gondwana: implications for the Gondwanan Carboniferous-Permian boundary. J. geol. Soc. Aust. 29:267-276.

Bailey, R.A., Dalrymple, G.B. and Lanphere, M.A. 1976. Volcanism, structure and geochronology of Long Valley caldera, Mono County, California. J. geophys. Res. 81:725-744.

Baker, M.C.W. 1977. Geochronology of upper Tertiary volcanic activity in the Andes of north Chile. Geol. Rdsch. 66:455-465.

Baker, M.C.W. 1981. The nature and distribution of Upper Cenozoic ignimbrite centres in the Central Andes. J. Volcanol. Geotherm. Res. 11:293-315.

Baker, M.C.W. and Francis, P.W. 1978. Upper Cenozoic volcanism in the Central Andes - ages and volumes. Earth Planet. Sci. Lett. 41:175-187.

Barazangi, M. and Isacks, B.L. 1976. Spatial distribution of earthquakes and subduction of the Nazca plate beneath South America. Geology 4:686-692.

Beanland, S. 1982. The Rotokawau Basalt. In: B.F. Houghton and I.E.M. Smith (Editors), New Zealand Volcanological Workshop, Handbook and Proceedings, 17 pp.

Beckett, J., Hamilton, D.S. and Weber, C.R. 1983. Permian and Triassic stratigraphy and sedimentation in the Gunnedah-Narrabri-Coonabarabran region. N.S.W. Geol. Surv., Q. Notes 51:1-16.

Bembrick, C., Herbert, C., Scheibner, E. and Stunz, J. 1980. Structural subdivision of the Sydney Basin. In: C. Herbert and R. Helby (Editors), A Guide to the Sydney Basin. Bull. geol. Surv. N.S.W. 26:2-9.

Bennett, F.D. 1972. Shallow submarine volcanism. J. geophys. Res. 77:5755-5759.

Benson, W.N. 1920. The geology and petrology of the Great Serpentine Belt of New South Wales. Part IX. The geology of the Currabubula district. Proc. Linn. Soc. N.S.W. 45:285-317.

Blank, H.R. 1965. Ash-flow deposits of the central King County, New Zealand. N.Z. Jl. Geol. Geophys. 8:588-607.

Bond, A. and Sparks, R.S.J. 1976. The Minoan eruption of Santorini, Greece. J. geol. Soc. Lond. 132:1-16.

Brazier, S., Sparks, R.S.J., Carey, S.N., Sigurdsson, H. and Westgate, J.A. 1983. Bimodal grain size distribution and secondary thickening in air-fall ash layers. Nature 301:115-119.

Briggs, N.D. 1976. Welding and crystallisation zonation in Whakamaru Ignimbrite, Central North Island, New Zealand. N.Z. Jl. Geol. Geophys. 19:189-212.

Brownlow, J.W. 1979. Discussion: the Reids Mistake Formation at Swansea Heads, New South Wales. J. geol. Soc. Aust. 26:319-322.

Brownlow, J.W. 1981. Early Permian sediments in the Maules Creek district, New South Wales. Geol. Soc. Aust., Coal Geology Group, Journal, 2:125-160.

Brunker, R.L. and Chesnut, W.S. 1976. Grafton 1:250,000 Geological Sheet. Geol. Surv. N.S.W., Sydney.

Butel, D., McLean, A. and Millar, A. 1983. Maules Creek - an interesting deposit. In: K.H.R. Moelle (Editor), Advances in the Study of the Sydney Basin, 17th Symposium, Programme and Abstracts. Newcastle University, N.S.W. pp. 34-35.

Byers, F.M., Carr, W.J., Orkild, P.P., Quinlivan, W.D. and Sargent, K.A. 1976. Volcanic suites and related cauldrons of Timber Mountain-Oasis Valley caldera complex, southern Nevada. Prof. Pap. U.S. geol. Surv. 919.

Cant, D.J. 1982. Fluvial facies models and their application. In: P.A. Scholle and D. Spearing (Editors), Sandstone Depositional Environments. AAPG, Oklahoma, pp. 115-137.

Carey, S.N. and Sigurdsson, H. 1980. The Roseau ash: deep-sea tephra deposits from a major eruption on Dominica, Lesser Antilles arc. J. Volcanol. Geotherm. Res. 7:67-86.

Carey, S.W. 1934. The geological structure of the Werrie Basin. Proc. Linn. Soc. N.S.W. 59:351-374.

Carey, S.W. 1935. Note on the Permian sequence in the Werrie Basin. Proc. Linn. Soc. N.S.W. 60:447-456.

Carey, S.W. 1937. The Carboniferous sequence in the Werrie Basin. Proc. Linn. Soc. N.S.W. 62:341-376.

Carey, S.W. and Browne, W.R. 1938. Review of the Carboniferous stratigraphy, tectonics and palaeogeography of New South Wales and Queensland. J. Proc. R. Soc. N.S.W. 71:591-614.

Cas, R.A.F. 1983. Submarine 'crystal tuffs': their origin using a Lower Devonian example from southeastern Australia. Geol. Mag. 120:471-486.

Cawood, P.A. 1982. Structural relations in the subduction complex of the Paleozoic New England Fold Belt, eastern Australia. J. Geol. 90:381-392.

Chapin, C.E. and Lowell, G.R. 1979. Primary and secondary flow structures in ash-flow tuffs of the Gribbles Run palaeovalley, central Colorado. In: C.E. Chapin and W.E. Elston (Editors), Ash-flow Tuffs. Spec. Pap. geol. Soc. Am. 180:137-154.

Chong, G. 1977. Contribution to the knowledge of the Domeyko Range in the Andes of Northern Chile. Geol. Rdsch. 66:374-403.

Christiansen, R.L. 1979. Cooling units and composite sheets in relation to caldera structure. In: C.E. Chapin and W.E. Elston (Editors), Ash-flow Tuffs. Spec. Pap. geol. Soc. Am. 180:29-42.

Christiansen, R.L. and Lipman, P.W. 1966. Emplacement and thermal history of a rhyolite lava flow near Fortymile Canyon, southern Nevada. Bull. geol. Soc. Am. 77:671-684.

Christiansen, R.L. and Blank, H.R. 1972. Volcanic stratigraphy of the Quaternary rhyolite plateau in Yellowstone National Park. Prof. Pap. U.S. geol. Surv. 729-B.

Christiansen, R.L. and Lipman, P.W. 1972. Cenozoic volcanism and plate-tectonic evolution of the western United States. II. Late Cenozoic. Philos. Trans. R. Soc. Lond. 271:249-284.

Christiansen, R.L., Lipman, P.W., Carr, W.J., Byers, F.M., Orkild, P.P. and Sargent, K.A. 1977. Timber Mountain-Oasis Valley caldera complex of southern Nevada. Bull. geol. Soc. Am. 88:943-959.

Clark, A.H., Mayer, A.E.S., Mortimer, C., Sillitoe, R.H., Cooke, R.U. and Snelling, N.J. 1967. Implications of the isotopic ages of ignimbrite flows, southern Atacama Desert, Chile. Nature 215:723-724.

Clough, B.J., Wright, J.V. and Walker, G.P.L. 1981. An unusual bed of giant pumice in Mexico. Nature 289:49-50.

Clough, B.J., Wright, J.V. and Walker, G.P.L. 1982. Morphology and dimensions of the young comendite lavas of La Primavera volcano, Mexico. Geol. Mag. 119:477-485.

Cole, J.W. 1970. Structure and eruptive history of the Tarawera Volcanic Complex. N.Z. Jl. Geol. Geophys. 13:879-902.

Colgate, S.A. and Sigurgeirsson, T. 1973. Dynamic mixing of water and lava. Nature 244:552-555.

Collinson, J.D. 1978a. Alluvial sediments. In: H.G. Reading (Editor), Sedimentary Environments and Facies. Blackwell Scientific Publications, pp. 15-60.

Collinson, J.D. 1978b. Lakes. In: H.G. Reading (Editor), Sedimentary Environments and Facies. Blackwell Scientific Publications, pp. 61-79.

Collinson, J.D. 1978c. Deserts. In: H.G. Reading (Editor), Sedimentary Environments and Facies. Blackwell Scientific Publications, pp. 80-97.

Collinson, J.D. and Thompson, D.B. 1982. Sedimentary Structures. George Allen and Unwin, London, 194 pp.

Conaghan, P.J., Jones, J.G., McDonnell, K.L. and Royce, K. 1982. A dynamic fluvial model for the Sydney Basin. J. geol. Soc. Aust. 29:55-70.

Coulon, C. and Thorpe, R.S. 1981. Role of continental crust in petrogenesis of orogenic volcanic associations. Tectonophys. 77:79-93.

Crandell, D.R. 1971. Postglacial lahars from Mount Rainier Volcano, Washington. Prof. Pap. U.S. geol. Surv. 677.

Crane, D.T. and Hunt, J.W. 1980. The Carboniferous sequence in the Gloucester-Myall Lake area New South Wales. J. geol. Soc. Aust. 26:341-352.

Crisci, G.M., De Rosa, R., Lanzafame, G., Mazzuoli, R., Sheridan, M.F. and Zuffa, G.G. 1981. Monte Guardia sequence: a Late-Pleistocene eruptive cycle on Lipari (Italy). Bull. Volcanol. 44:241-255.

Crook, K.A.W. 1980a. Fore-arc evolution and continental growth: a general model. J. Struct. Geol. 2:289-303.

Crook, K.A.W. 1980b. Fore-arc evolution in the Tasman Geosyncline: the origin of the southeast Australian continental crust. J. geol. Soc. Aust. 27:215-232.

Crook, K.A.W. and Powell, C.McA. 1976. The evolution of the southeastern part of the Tasman Geosyncline. 25th Int. geol. Congr., Field Guide, Excursion 17A.

Crowe, B.M. and Fisher, R.V. 1973. Sedimentary structures in base-surge deposits with special reference to cross-bedding, Ubehebe Craters, Death Valley, California. Bull. geol. Soc. Am. 84:663-682.

Crowell, J.C. and Frakes, L.A. 1971a. Late Palaeozoic glaciation of Australia. J. geol. Soc. Aust. 17:115-155.

Crowell, J.C. and Frakes, L.A. 1971b. Late Palaeozoic glaciation: part IV, Australia. Bull. geol. Soc. Am. 82:2515-2540.

Cuddy, R.G. 1978. Internal structures and tectonic setting of part of the New England Batholith and associated volcanic rocks, northern New South Wales. Unpub. Ph.D. Thesis, University of New England, Armidale.

Curtis, G.H. 1968. The stratigraphy of the ejecta from the 1912 eruption of Mount Katmai and Novarupta, Alaska. In: R.R. Coats and others (Editors), Studies in Volcanology. Mem. geol. Soc. Am. 116:153-210.

Davies, D.K., Vessell, R.K., Miles, R.C., Foley, M.G. and Bonis, S.B. 1978. Fluvial transport and downstream sediment modifications in an active volcanic region. In: A.D. Miall (Editor), Fluvial Sedimentology. Canadian Society of Petroleum Geologists, Alberta, Canada, pp. 61-84.

Day, R.W., Murray, C.G. and Whitaker, W.G. 1978. The eastern part of the Tasman Orogenic Zone. Tectonophys. 48:327-364.

Deal, E.G., Elston, W.E., Erb, E.E., Peterson, S.L., Reiter, D.E., Damon, P.E. and Shafiqullah, M. 1978. Cenozoic volcanic geology of the Basin and Range province in Hidalgo County, southwesternmost New Mexico: progress report no. 1. New Mex. geol. Soc., Guidebook of Land of Cochise, 29th Field Conference, pp. 219-229.

Deruelle, B. 1978. Calc-alkaline and shoshonitic lavas from five Andean volcanoes (between latitudes 21°45' and 24°30'S) and the distribution of the Plio-Quaternary volcanism of the south-central and southern Andes. J. Volcanol. Geotherm. Res. 3:281-298.

Deruelle, B. 1982. Petrology of the Plio-Quaternary volcanism of the South-Central and Meridional Andes. J. Volcanol. Geotherm. Res. 14:77-124.

Dickinson, W.R. 1970. Relations of andesites, granites and derivative sandstones to arc-trench tectonics. Rev. Geophysics Space Physics 8:813-860.

Dickinson, W.R. and Seely, D.R. 1979. Structure and stratigraphy of forearc regions. Bull. AAPG 63:2-31.

Dingman, R.J. 1965. Pliocene age of the ash-flow deposits of the San Pedro area, Chile. Prof. Pap. U.S. geol. Surv. 525-C:63-67.

Doell, R.R., Dalrymple, G.B., Smith, R.L. and Bailey, R.A. 1968. Paleomagnetism, potassium-argon ages, and geology of rhyolites and associated rocks of the Valles caldera, New Mexico. In: R.R. Coats and others (Editors), Studies in Volcanology. Mem. geol. Soc. Am. 116:211-248.

Druitt, T.H. and Sparks, R.S.J. 1982. A proximal ignimbrite breccia facies on Santorini, Greece. J. Volcanol. Geotherm. Res. 13:147-171.

Eaton, G.P., Christiansen, R.L., Iyer, H.M., Pitt, A.M., Mabey, D.R., Blank, H.R., Zietz, I. and Gettings, M.E. 1975. Magma beneath Yellowstone National Park. Science 188:787-796.

Ekren, E.B. and Byers, F.M. 1976. Ash-flow fissure vent in west-central Nevada. Geology 4:247-251.

Elston, W.E. 1978. Mid-Tertiary cauldrons and their relationship to mineral resources, southwestern New Mexico: a brief review. In: C.E. Chapin and W.E. Elston (Editors), Field Guide to Selected Cauldrons and Mining Districts of the Datil-Mogollon Volcanic Field New Mexico. New Mex. geol. Soc., Spec. Publ. 7:107-113.

Elston, W.E. 1984. Mid-Tertiary ash-flow tuff cauldrons, southwestern New Mexico. J. geophys. Res. in press.

Elston, W.E. and Bornhorst, T.J. 1979. The Rio Grande rift in context of regional post-40 M.Y. volcanic and tectonic events. In: R.E. Riecker (Editor), Rio Grande Rift: Tectonics and Magmatism. American Geophysical Union, pp. 416-438.

Elston, W.E., Rhodes, R.C., Coney, P.J. and Deal, E.G. 1976. Progress report on the Mogollon Plateau volcanic field, southwestern New Mexico, no. 3 - Surface expression of a pluton. In: W.E. Elston and S.A. Northrop (Editors), Cenozoic Volcanism in Southwestern New Mexico. New Mex. geol. Soc., Spec. Publ. 5:3-28.

Evernden, J.F. and Richards, J.R. 1962. Potassium-argon ages in eastern Australia. J. geol. Soc. Aust. 9:1-50.

Ewart, A. 1979. A review of the mineralogy and chemistry of Tertiary-Recent dacitic, latitic, rhyolitic, and related salic volcanic rocks. In: F. Barker (Editor), Trondhjemites, Dacites and Related Rocks. Elsevier, Amsterdam, pp. 13-121.

Ewart, A. 1982. The mineralogy and petrology of Tertiary-Recent orogenic volcanic rocks: with special reference to the andesitic-basaltic compositional range. In: R.S. Thorpe (Editor), Andesites. John Wiley and Sons, pp. 25-87.

Ewart, A. and Le Maitre, R.W. 1980. Some regional compositional differences within Tertiary-Recent orogenic magmas. Chem. Geol. 30:257-283.

Exon, N.F. 1974. The geological evolution of the southern Taroom Trough and the overlying Surat Basin. J. Aust. Pet. Explor. Assoc. 14:50-58.

Facer, R.A. 1978. New and recalculated radiometric data supporting a Carboniferous age for the emplacement of the Bathurst Batholith, New South Wales. J. geol. Soc. Aust. 25:429-432.

Fenner, C.N. 1948. Incandescent tuff flows in southern Peru. Bull. geol. Soc. Am. 59:879-893.

Fergusson, C.L. 1982. An ancient accretionary terrain in eastern New England - evidence from the Coffs Harbour Block. In: P.G. Flood and B. Runnegar (Editors), New England Geology. Department of Geology, University of New England and AHV Club, Armidale, pp. 63-70.

Fergusson, C.L. 1984a. The Gundahl Complex of the New England Fold Belt, eastern Australia: a tectonic mélange formed in a Palaeozoic subduction complex. J. Struct. Geol. 6:257-271.

Fergusson, C.L. 1984b. Tectono-stratigraphy of a Palaeozoic subduction complex in the central Coffs Harbour Block of north-eastern New South Wales. Aust. J. Earth Sciences 31:217-236.

Fink, J.H. 1980a. Surface folding and viscosity of rhyolite flows. Geology 8:250-254.

Fink, J.H. 1980b. Gravity instability in the Holocene Big and Little Glass Mountain rhyolitic obsidian flows, northern California. Tectonophys. 66:147-166.

Fink, J.H. 1983. Structure and emplacement of a rhyolitic obsidian flow: Little Glass Mountain, Medicine Lake Highland, northern California. Bull. geol. Soc. Am. 94:362-380.

Fink, J.H. and Pollard, D.D. 1983. Structural evidence for dikes beneath silicic domes, Medicine Lake Highland volcano, California. Geology 11:458-461.

Fisher, R.V. 1961. Proposed classification of volcaniclastic sediments and rocks. Bull. geol. Soc. Am. 72:1409-1414.

Fisher, R.V. 1964. Maximum size, median diameter and sorting of tephra. J. geophys. Res. 69:341-355.

Fisher, R.V. 1977. Erosion by volcanic base-surge density currents: U-shaped channels. Bull. geol. Soc. Am. 88:1287-1297.

Fisher, R.V. 1979. Models for pyroclastic surges and pyroclastic flows. J. Volcanol. Geotherm. Res. 6:305-318.

Fisher, R.V. and Waters, A.C. 1970. Base surge bed forms in maar volcanoes. Am. J. Sci. 268:157-180.

Flood, P.G. and Fergusson, C.L. 1982. Tectono-stratigraphic units and structure of the Texas-Coffs Harbour region. In: P.G. Flood and B. Runnegar (Editors), New England Geology. Department of Geology, University of New England and AHV Club, pp. 71-78.

Flood, P.G. and Fergusson, C.L. 1984. The geological development of the northern New England Province of the New England Fold Belt. In: H.K. Herbert and J.M.W. Rynn (Editors), Volcanics, Granites and Mineralisation of the Stanthorpe-Emmaville-Drake Region. Geol. Soc. Aust., Queensl. Div. pp. 1-19.

Flood, R.H., Vernon, R.H., Shaw, S.E. and Chappell, B.W. 1977. Origin of pyroxene-plagioclase aggregates in a rhyodacite. Contr. Mineral. Petrol. 60:299-309.

Francis, P.W. and Rundle, C.C. 1976. Rates of production of the main magma types in the central Andes. Bull. geol. Soc. Am. 87:474-480.

Francis, P.W. and Baker, M.C.W. 1977. Mobility of pyroclastic flows. Nature 270:164-165.

Francis, P.W. and Baker, M.C.W. 1978. Sources of two large ignimbrites in the Central Andes: some LANDSAT evidence. J. Volcanol. Geotherm. Res. 4:81-87.

Francis, P.W., Roobol, M.J. and Walker, G.P.L. 1974. The San Pedro and San Pablo volcanoes of northern Chile and their hot avalanche deposits. Geol. Rdsch. 63:357-388.

Francis, P.W., Moorbath, S. and Thorpe, R.S. 1977. Strontium isotope data for Recent andesites in Ecuador and North Chile. Earth Planet. Sci. Lett. 37:197-202.

Francis, P.W., Halls, C. and Baker, M.C.W. 1983. Relationships between mineralization and silicic volcanism in the Central Andes. J. Volcanol. Geotherm. Res. 18:165-190.

Francis, P.W., Hammill, M., Kretzschmar, G. and Thorpe, R.S. 1978. The Cerro Galan caldera, north-west Argentina and its tectonic setting. Nature 274:749-751.

Fransen, P.J.B. and Briggs, R.M. 1981. Ignimbrites at Karapiro-Putaruru. In: R.M. Briggs (Compiler), Field Excursions Guide Book, Hamilton Conference. Geological Society of New Zealand Inc., pp. 29-34.

Froggatt, P.C. 1981. Stratigraphy and nature of the Taupo Pumice Formation. N.Z. Jl. Geol. Geophys. 24:231-248.

Gloppen, T.G. and Steel, R.J. 1981. The deposits, internal structure and geometry in six alluvial fan-fan delta bodies (Devonian-Norway) - a study in the significance of bedding sequence in conglomerates. In: F.G. Ethridge and R.M. Flores (Editors), Recent and Ancient Nonmarine Depositional Environments: Models for Exploration. SEPM Spec. Publ. 31:49-69.

Godden, N.L. 1982. The volcanic-plutonic association, Tenterfield region, New South Wales. In: P.G. Flood and B. Runnegar (Editors), New England Geology. Department of Geology, University of New England and AHV Club, pp. 211-219.

Green, T.H. 1980. Island arc and continent-building magmatism - a review of petrogenetic models based on experimental petrology and geochemistry. Tectonophys. 63:367-385.

Guest, J.E. 1969. Upper Tertiary ignimbrites in the Andean Cordillera of part of the Antofagasta Province, northern Chile. Bull. geol. Soc. Am. 80:337-362.

Guest, J.E. and Sanchez, J. 1969. A large dacitic lava flow in northern Chile. Bull. Volcanol. 33:778-790.

Hanlon, F.N. 1947a. Geology of the north-western coalfield. Part I. Geology of the Willow Tree district. J. Proc. R. Soc. N.S.W. 81: 280-286.

Hanlon, F.N. 1947b. Geology of the north-western coalfield. Part II. Geology of the Willow Tree-Temi district. J. Proc. R. Soc. N.S.W. 81:287-291.

Hanlon, F.N. 1947c. Geology of the north-western coalfield. Part III. Geology of the Murrurundi-Temi district. J. Proc. R. Soc. N.S.W. 81:292-297.

Hanlon, F.N. 1948a. Geology of the north-western coalfield. Part IV. Geology of the Gunnedah-Curlewis district. J. Proc. R. Soc. N.S.W. 82:241-250.

Hanlon, F.N. 1948b. Geology of the north-western coalfield. Part VI. Geology of the south-western part of County Nandewar. J. Proc. R. Soc. N.S.W. 82:255-261.

Hanlon, F.N. 1949. Geology of the north-western coalfield. Part XIX. Geology of the Boggabri district. J. Proc. R. Soc. N.S.W. 82:297-301.

Harrington, H.J. 1974. The Tasman geosyncline in Australia. In: A.K. Denmead, G.W. Tweedale and A.F. Wilson (Editors), The Tasman Geosyncline - a Symposium. Geol. Soc. Aust., Queensl. Div. pp. 383-407.

Harrington, H.J. 1982. Tectonics and the Sydney Basin. In: D.R. Offler (Editor), Advances in the Study of the Sydney Basin, 16th Symposium, Programme and Abstracts. Newcastle University, N.S.W. pp. 15-19.

Heiken, G.H. 1971. Tuff rings: examples from the Fort Rock-Christmas Lake Valley Basin, south-central Oregon. J. geophys. Res. 76:5615-5626.

Heiken, G.H. 1972. Morphology and petrography of volcanic ashes. Bull. geol. Soc. Am. 83:1961-1988.

Heiken, G. and Goff, F. 1983. Hot dry rock geothermal energy in the Jemez volcanic field, New Mexico. J. Volcanol. Geotherm. Res. 15:223-246.

Heiken, G., Crowe, B., McGetchin, T., West, F., Eichelberger, J., Bartram, D., Peterson, R. and Wohletz, K. 1980. Phreatic eruption clouds: the activity of La Soufrière de Guadeloupe, F.W.I., August-October, 1976. Bull. Volcanol. 43:383-395.

Herbert, C. 1980. Evidence for glaciation in the Sydney Basin and Tamworth Synclinorial Zone. In: C. Herbert and R. Helby (Editors), A Guide to the Sydney Basin. Bull. geol. Surv. N.S.W. 26:274-293.

Hildreth, W. 1981. Gradients in silicic magma chambers: implications for lithospheric magmatism. J. geophys. Res. 86:10153-10192.

Hildreth, W. 1983. The compositionally zoned eruption of 1912 in the Valley of Ten Thousand Smokes, Katmai National Park, Alaska. J. Volcanol. Geotherm. Res. 18:1-56.

Hildreth, W., Grunder, A.L. and Drake, R.E. 1984. The Loma Seca Tuff and the Calabozos caldera: a major ash-flow and caldera complex in the southern Andes of central Chile. Bull. geol. Soc. Am. 95:45-54.

Hoblitt, R.P., Miller, C.D. and Vallance, J.W. 1981. Origin and stratigraphy of the deposit produced by the May 18 directed blast. In: P.W. Lipman and D.R. Mullineaux (Editors), The 1980 Eruptions of Mount St. Helens, Washington. Prof. Pap. U.S. geol. Surv. 1250:401-419.

Hollingworth, S.E. and Guest, J.E. 1967. Pleistocene glaciation in the Atacama Desert, northern Chile. J. Glaciology 6:749-751.

Hollingworth, S.E. and Rutland, R.W.R. 1968. Studies of Andean uplift Part I - post-Cretaceous evolution of the San Bartolo area, north Chile. Geol. J. 6:49-62.

Honnorez, J. and Kirst, P. 1975. Submarine basaltic volcanism: morphometric parameters for discriminating hyaloclastites from hyalotuffs. Bull. Volcanol. 39:441-465.

Houghton, B.F., Scott, F.J., Nairn, I.A. and Wood, C.P. 1983. Cyclic variation in eruption products, White Island Volcano, New Zealand 1976-79 (Note). N.Z. Jl. Geol. Geophys. 26:213-216.

Hulme, G. 1974. The interpretation of lava flow morphology. Geophys. J. R. astr. Soc. 39:361-383.

Hume, T.M., Sherwood, A.M. and Nelson, C.S. 1975. Alluvial sedimentology of the Upper Pleistocene Hinuera Formation, Hamilton Basin, New Zealand. N.Z. Jl. Geol. Geophys. 5:421-462.

Hunt, J.W., Brakel, A.T. and Harrington, H.J. 1983. Coal quality and geological setting in the Early Permian Sydney and Gunnedah Basins. In: K.H.R. Moelle (Editor), Advances in the Study of the Sydney Basin, 17th Symposium, Programme and Abstracts. Newcastle University, N.S.W. pp. 36-39.

Huppert, H.E., Shepherd, J.B., Sigurdsson, H. and Sparks, R.S.J. 1982. On lava dome growth, with application to the 1979 lava extrusion on the Soufrière of St. Vincent. J. Volcanol. Geotherm. Res. 14:199-222.

Irvine, T.N. and Baragar, W.R.A. 1971. A guide to the chemical classification of the common volcanic rocks. Can. J. Earth Sci. 8:523-548.

Irving, E. 1966. Paleomagnetism of some Carboniferous rocks from New South Wales and its relation to geological events. J. geophys. Res. 71:6025-6051.

James, D.E. 1971. Plate tectonic model for the evolution of the central Andes. Bull. geol. Soc. Am. 82:3325-3346.

Janda, R.J., Scott, K.M., Nolan, K.M. and Martinson, H.A. 1981. Lahar movement, effects, and deposits. In: P.W. Lipman and D.R. Mullineaux (Editors), The 1980 Eruptions of Mount St. Helens, Washington. Prof. Pap. U.S. geol. Surv. 1250:461-478.

Jordan, T.E., Isacks, B.L., Allmendinger, R.W., Brewer, J.A., Ramos, V.A. and Ando, C.J. 1983. Andean tectonics related to geometry of subducted Nazca plate. Bull. geol. Soc. Am. 94:341-361.

Karig, D.E. and Sharman, G.F. 1975. Subduction and accretion in trenches. Bull. geol. Soc. Am. 86:377-389.

Katz, H.R. 1971. Continental margin in Chile - is tectonic style compressional or extensional? Bull. AAPG 55:1753-1758.

Kemp, E.M., Balme, B.E., Helby, R.J., Playford, G. and Price, P.L. 1977. Carboniferous and Permian palynostratigraphy in Australia and Antarctica: a review. Bur. Miner. Resour. J. Aust. Geol. Geophys. 2:177-208.

Kienle, J., Kyle, P.R., Self, S., Motyka, R.J. and Lorenz, V. 1980. Ukinrek Maars, Alaska, I. April 1977 eruption sequence, petrology and tectonic setting. J. Volcanol. Geotherm. Res. 7:11-37.

Kokelaar, B.P. 1983. The mechanism of Surtseyan volcanism. J. geol. Soc. Lond. 140:939-944.

Korringa, M.K. 1973. Linear vent area of the Soldier Meadow Tuff, an ash-flow sheet in northwestern Nevada. Bull. geol. Soc. Am. 84:3849-3866.

Korsch, R.J. 1977. A framework for the Palaeozoic geology of the southern part of the New England Geosyncline. J. geol. Soc. Aust. 25:339-355.

Korsch, R.J. 1978. Petrographic variations within thick turbidite sequences: an example from the late Palaeozoic of eastern Australia. Sedimentology 25:247-265.

Korsch, R.J. 1984. Sandstone compositions from the New England Orogen, eastern Australia: implications for tectonic setting. J. sediment. Petrol. 54:192-211.

Korsch, R.J. and Harrington, H.J. 1981. Stratigraphic and structural synthesis of the New England Orogen. J. geol. Soc. Aust. 28:205-226.

Korsch, R.J., Archer, N.R. and McConachy, G.W. 1978. The Demon Fault. J. Proc. R. Soc. N.S.W. 111:101-106.

Kortemeier, C.P. and Sheridan, M.F. 1983. Role of grain type in quantitative surface morphology of pyroclasts from the Monte Guardia sequence on Lipari, Italy. In: R. Gooley (Editor), Microbeam Analysis - 1983. San Francisco Press Inc., San Francisco, pp. 43-46.

Kuno, H., Ishikawa, T., Katsui, Y., Yagi, K., Yamasaki, M. and Taneda, S. 1964. Sorting of pumice and lithic fragments as a key to eruptive and emplacement mechanism. Jap. J. Geol. Geogr. 35:223-238.

Kussmaul, S., Hörmann, P.K., Ploskonka, E. and Subieta, T. 1977. Volcanism and structure of southwestern Bolivia. J. Volcanol. Geotherm. Res. 2:73-111.

Lahsen, A. 1982. Upper Cenozoic volcanism and tectonism in the Andes of northern Chile. Earth Sci. Rev. 18:285-302.

Ledbetter, M.T. and Sparks, R.S.J. 1979. Duration of large-magnitude explosive eruptions deduced from graded bedding in deep-sea ash layers. Geology 7:240-244.

Leeman, W.P. 1983. The influence of crustal structure on compositions of subduction-related magmas. J. Volcanol. Geotherm. Res. 18:561-588.

Leitch, E.C. 1969. Igneous activity and diastrophism in the Permian of New South Wales. Geol. Soc. Aust., Spec. Publ. 2:21-37.

Leitch, E.C. 1974. The geological development of the southern part of the New England Fold Belt. J. geol. Soc. Aust. 21:133-156.

Leitch, E.C. 1975. Plate tectonic interpretation of the Paleozoic history of the New England Fold Belt. Bull. geol. Soc. Am. 86:141-144.

Leitch, E.C. and Willis, S.G.A. 1982. Nature and significance of plutonic clasts in Devonian conglomerates of the New England Fold Belt. J. geol. Soc. Aust. 29:83-89.

Lindsay, J.F. 1969. The glacial origin of Carboniferous conglomerates west of Barraba, New South Wales: discussion. Bull. geol. Soc. Am. 80:911-914.

Lipman, P.W. 1975. Evolution of Platoro caldera complex and related volcanic rocks, southeastern San Juan Mountains, Colorado. Prof. Pap. U.S. geol. Surv. 852.

Lipman, P.W. 1976. Caldera-collapse breccias in the western San Juan Mountains, Colorado. Bull. geol. Soc. Am. 87:1397-1410.

Lipman, P.W., Steven, T.A., Luedke, R.G. and Burbank, W.S. 1973. Revised volcanic history of the San Juan, Uncompahgre, Silverton, and Lake City calderas in the western San Juan Mountains, Colorado. J. Res. U.S. geol. Surv. 1:627-642.

Lipman, P.W., Doe, B.R., Hedge, C.E. and Steven, T.A. 1978. Petrologic evolution of the San Juan volcanic field southwestern Colorado: Pb and Sr isotope evidence. Bull. geol. Soc. Am. 89:59-82.

Lipman, P.W., Fisher, F.S., Mehnert, H.H., Naeser, C.W., Luedke, R.G. and Steven, T.A. 1976. Multiple ages of mid-Tertiary mineralization and alteration in the western San Juan Mountains, Colorado. Econ. Geol. 71:571-588.

Loney, R.A. 1968. Flow structure and composition of the Southern Coulee, Mono Craters, California - a pumiceous rhyolite flow. In: R.R. Coats and others (Editors), Studies in Volcanology. Mem. geol. Soc. Am. 116:415-440.

Lorenz, V. 1970. Some aspects of the eruption mechanism of the Big Hole Maar, central Oregon. Bull. geol. Soc. Am. 81:1823-1830.

Lorenz, V. 1973. On the formation of maars. Bull. Volcanol. 37:183-204.

Lorenz, V. 1974. Vesiculated tuffs and associated features. Sedimentology 21:273-291.

Loughnan, F.C. 1973. Kaolinite clayrocks of the Koogah Formation, New South Wales. J. geol. Soc. Aust. 20:329-341.

Loughnan, F.C. 1975. Correlatives of the Greta Coal Measures in the Hunter Valley and the Gunnedah Basin, New South Wales. J. geol. Soc. Aust. 22:243-253.

Lowe, D.R. and Lo Piccolo, R.D. 1974. The characteristics and origins of dish and pillar structures. J. sediment. Petrol. 44:484-501.

Lowe, S.P. 1971. Stratigraphy of the Willow Tree district, New South Wales. Unpubl. B.Sc. (Hons) Thesis, University of New England, Armidale.

Luedke, R.G. and Burbank, W.S. 1968. Volcanism and cauldron development in the western San Juan Mountains, Colorado. In: R.R. Coats and others (Editors), Studies in Volcanology. Mem. geol. Soc. Am. 116:175-208.

Mahood, G.A. 1980. Geological evolution of a Pleistocene rhyolitic center - Sierra La Primavera, Jalisco, Mexico. J. Volcanol. Geotherm. Res. 8:199-230.

Manser, W. 1965a. Geological Map of New England 1:100 000 Curlewis Sheet (no. 330), with marginal text. University of New England, Armidale, N.S.W., Australia.

Manser, W. 1965b. Geological Map of New England 1:100 000 Gunnedah Sheet (no. 320), with marginal text. University of New England, Armidale, N.S.W., Australia.

Manser, W. 1968. Geological Map of New England 1:100 000 Wingen Sheet (no. 359), with marginal text. University of New England, Armidale, N.S.W., Australia.

Martin, H. 1981. The late Palaeozoic Gondwana glaciation. Geol. Rdsch. 70:480-498.

McClung, G. 1980. Permian marine sedimentation in the northern Sydney Basin. In: C. Herbert and R. Helby (Editors), A Guide to the Sydney Basin. Bull. geol. Surv. N.S.W. 26:54-72.

McKee, E.D., Crosby, E.J. and Berryhill, H.L. 1967. Flood deposits, Bijou Creek, Colorado, June 1965. J. sediment. Petrol. 37:829-851.

McKee, E.H. 1970. Fish Creek Mountains Tuff and volcanic center, Lander County, Nevada. Prof. Pap. U.S. geol. Surv. 681.

McKee, E.H. 1979. Ash-flow sheets and calderas: their genetic relationship to ore deposits in Nevada. In: C.E. Chapin and W.E. Elston (Editors), Ash-flow Tuffs. Spec. Pap. geol. Soc. Am. 180:205-211.

McKelvey, B.C. 1968. Geological Map of New England 1:100 000 Bangheet (no. 280), with marginal text. University of New England, Armidale, N.S.W., Australia.

McKelvey, B.C. 1974. Devonian and Carboniferous sedimentation on the Tamworth Shelf. In: C.G. Murray and B. Runnegar (Editors), Field Conference, New England Area. Geol. Soc. Aust., Queensl. Div. pp. 20-22.

McKelvey, B.C. and White, A.H. 1964. Geological Map of New England 1:100 000 Horton Sheet (no. 290), with marginal text. University of New England, Armidale, N.S.W., Australia.

McKelvey, B.C. and Gutsche, H.W. 1969. The geology of some Permian sequences on the New England Tablelands, New South Wales. Geol. Soc. Aust., Spec. Publ. 2:13-20.

McPhie, J. 1982. The Coombadjha Volcanic Complex: a Late Permian cauldron, northeastern New South Wales. In: P.G. Flood and B. Runnegar (Editors), New England Geology. Department of Geology, University of New England and AHV Club, pp. 221-227.

McPhie, J. 1983. Outflow ignimbrite sheets from Late Carboniferous calderas, Currabubula Formation, New South Wales, Australia. Geol. Mag. 120:487-503.

McPhie, J. 1984. Permo-Carboniferous silicic volcanism and palaeogeography on the western edge of the New England Orogen, northeastern New South Wales. Aust. J. Earth Sciences 31:133-146.

McPhie, J. and Fergusson, C.L. 1983. Dextral movement on the Demon Fault, northeastern New South Wales: a reassessment. J. Proc. R. Soc. N.S.W. 116:123-127.

Megard, F. and Philip, H. 1976. Plio-Quaternary tectono-magmatic zonation and plate tectonics in the central Andes. Earth Planet. Sci. Lett. 33:231-238.

Miall, A.D. 1977. A review of the braided-river depositional environment. Earth Sci. Rev. 13:1-62.

Miall, A.D. 1978. Lithofacies types and vertical profile models in braided river deposits: a summary. In: A.D. Miall (Editor), Fluvial Sedimentology. Canadian Society of Petroleum Geologists, Alberta, Canada, pp. 597-604.

Moore, D. and Roberts, J. 1976. The Early Carboniferous marine transgression in the Merlewood Formation, Werrie Syncline, New South Wales. J. Proc. R. Soc. N.S.W. 109:49-57.

Moore, J.G. 1967. Base surge in recent volcanic eruptions. Bull. Volcanol. 30:338-363.

Moore, J.G. and Peck, D.L. 1962. Accretionary lapilli in volcanic rocks of the western continental United States. J. Geol. 70:182-193.

Moore, J.G., Nakamura, K. and Alcaraz, A. 1966. The 1965 eruption of Taal Volcano. Science 151:955-960.

Moore, P.R. 1983. Rhyolite domes and pyroclastic rocks (Whitianga Group) of the Hahei area, Coromandel Peninsula. J.R. Soc. N.Z. 13:79-92.

Mortimer, C. 1973. The Cenozoic history of the southern Atacama Desert, Chile. J. geol. Soc. Lond. 129:505-526.

Mortimer, C. and Saric, N. 1975. Cenozoic studies in northernmost Chile. Geol. Rdsch. 64:395-420.

Mory, A.J. 1981. A review of Early Carboniferous stratigraphy and correlations in the northern Tamworth Belt, New South Wales. Proc. Linn. Soc. N.S.W. 105:213-236.

Mory, A.J. 1982. The Early Carboniferous palaeogeography of the northern Tamworth Belt, New South Wales. J. geol. Soc. Aust. 29:357-366.

Murray, C.G. 1983. Permian geology of Queensland. In: Permian Geology of Queensland. Geol. Soc. Aust., Queensl. Div. pp. 1-32.

Murray, C.G. and Whitaker, W.G. 1982. A review of the stratigraphy, structure and regional tectonic setting of the Brisbane Metamorphics. In: P.G. Flood and B. Runnegar (Editors), New England Geology. Department of Geology, University of New England and AHV Club, pp. 79-94.

Nairn, I.A. 1976. Atmospheric shock waves and condensation clouds from Ngauruhoe explosive eruptions. Nature 259:190-192.

Nairn, I.A. 1982. The Okataina Volcanic Centre. In: B.F. Houghton and I.E.M. Smith (Editors), New Zealand Volcanological Workshop, Handbook and Proceedings, pp. 1-16.

Nairn, I.A. and Wiradiradjha, S. 1980. Late Quaternary hydrothermal explosion breccias at Kawerau geothermal field, New Zealand. Bull. Volcanol. 43:1-13.

Nasher, B., Engel, B.A. and McKnight, S.W. 1976. Hunter Valley: Carboniferous geology. 25th Int. geol. Congr., Field Guide, Excursion 10B.

Nathan, S. (Compiler) 1976. Volcanic and geothermal geology of the central North Island, New Zealand. 25th Int. geol. Congr., Field Guide, Excursions 55A and 56A.

Newhall, C.G. and Self, S. 1982. The volcanic explosivity index (VEI): an estimate of explosive magnitude for historical volcanism. J. geophys. Res. 87:1231-1238.

Newhall, C.G. and Melson, W.G. 1983. Explosive activity associated with the growth of volcanic domes. J. Volcanol. Geotherm. Res. 17:111-131.

Nilsen, T.H. 1982. Alluvial fan deposits. In: P.A. Scholle and D. Spearing (Editors), Sandstone Depositional Environments. AAPG, Oklahoma, pp. 49-86.

Ninkovich, D., Sparks, R.S.J. and Ledbetter, M.T. 1978. The exceptional magnitude and intensity of the Toba eruption, Sumatra: an example of the use of deep-sea tephra layers as a geological tool. Bull. Volcanol. 41:286-298.

Noble, D.C., McKee, E.H., Farrar, E. and Petersen, U. 1974. Episodic Cenozoic volcanism and tectonism in the Andes of Peru. Earth Planet. Sci. Lett. 21:213-220.

Olgers, F., Flood, P.G. and Robertson, A.D. 1974. Palaeozoic geology of the Warwick and Goondiwindi 1:250 000 Sheet areas, Queensland and New South Wales. Bur. Miner. Resour. Geol. Geophys. Aust., Report 164, 109 pp.

Packham, G.H. 1969. The general features of the geological provinces of New South Wales. In: G.H. Packham (Editor), The Geology of New South Wales. J. geol. Soc. Aust. 16:1-17.

Palacios, M.C. 1984. Considerations about the plate tectonic model, volcanism and continental crust in the southern part of the Central Andes. Tectonophys. 106:205-214.

Paskoff, R.P. 1977. Quaternary of Chile: the state of research. Quaternary Research 8:2-31.

Peccerillo, A. and Taylor, S.R. 1976. Geochemistry of Eocene calc-alkaline volcanic rocks from the Kastamonu area, northern Turkey. Contr. Mineral. Petrol. 58:63-81.

Peckover, R.S., Buchanan, D.J. and Ashby, D.E.T.F. 1973. Fuel-coolant interactions in submarine volcanism. Nature 245:307-308.

Pichler, H. and Zeil, W. 1972. The Cenozoic rhyolite-andesite association of the Chilean Andes. Bull. Volcanol. 36:424-452.

Pogson, D.J. and Hitchins, B.L. 1973. New England 1:500,000 Geological Sheet. Geol. Surv. N.S.W., Sydney.

Pogson, D.J. and Scheibner, E. 1976. Palaeozoic accretion of eastern Australia. 25th Int. geol. Congr., Field Guide, Excursion 16A.

Powell, C.McA. and Edgecombe, D.R. 1978. Mid-Devonian movements in the northeastern Lachlan Fold Belt. J. geol. Soc. Aust. 25:165-184.

Powell, C.McA., Edgecombe, D.R., Henry, N.M. and Jones, J.G. 1976. Timing of regional deformation of the Hill End Trough: a reassessment. J. geol. Soc. Aust. 23:407-421.

Price, I. 1973. A new Permian and Upper Carboniferous (?) succession near Woodsreef, N.S.W., and its bearing on the palaeogeography of western New England. Proc. Linn. Soc. N.S.W. 97:202-210.

Ragan, D.M. and Sheridan, M.F. 1972. Compaction of the Bishop Tuff, California. Bull. geol. Soc. Am. 83:95-106.

Ramsay, W.R.H. and Stanley, J.M. 1976. Magnetic anomalies over the western margin of the New England foldbelt, northeast New South Wales. Bull. geol. Soc. Am. 87:1421-1428.

Ratté, J.C. and Steven, T.A. 1967. Ash flows and related volcanic rocks associated with the Creede caldera, San Juan Mountains, Colorado. Prof. Pap. U.S. geol. Surv. 524-H.

Rhodes, R.C. 1976a. Volcanic geology of the Mogollon Range and adjacent areas, Catron and Grant Counties, New Mexico. In: W.E. Elston and S.A. Northrop (Editors), Cenozoic Volcanism in Southwestern New Mexico. New Mex. geol. Soc., Spec. Publ. 5:42-50.

Rhodes, R.C. 1976b. Petrologic framework of the Mogollon Plateau volcanic ring complex, New Mexico - surface expression of a major batholith. In: W.E. Elston and S.A. Northrop (Editors), Cenozoic Volcanism in Southwestern New Mexico. New Mex. geol. Soc., Spec. Publ. 5:103-112.

Rhodes, R.C. and Smith, E.I. 1972. Geology and tectonic setting of the Mule Creek caldera, New Mexico, U.S.A. Bull. Volcanol. 36:401-411.

Roberts, J. and Engel, B.A. 1980. Carboniferous palaeogeography of the Yarrol and New England Orogens, eastern Australia. J. geol. Soc. Aust. 27:167-186.

Roobol, M.J. and Smith, A.L. 1976. Mount Pelée, Martinique: a pattern of alternating eruptive styles. Geology 4:521-524.

Rose, W.I. 1973. Pattern and mechanism of volcanic activity at the Santiaguito volcanic dome, Guatemala. Bull. Volcanol. 37:73-94.

Rose, W.I., Pearson, T. and Bonis, S. 1977. Nuée ardente eruption from the foot of a dacite lava flow, Santiaguito volcano, Guatemala. Bull. Volcanol. 40:23-38.

Ross, C.S. and Smith, R.L. 1961. Ash-flow tuffs: their origin, geologic relations, and identification. Prof. Pap. U.S. geol. Surv. 366.

Rowley, P.D., Kuntz, M.A. and Macleod, N.S. 1981. Pyroclastic flow deposits. In: P.W. Lipman and D.R. Mullineaux (Editors), The 1980 Eruptions of Mount St. Helens, Washington. Prof. Pap. U.S. geol. Surv. 1250:489-512.

Runnegar, B.N. 1970. The Permian faunas of northern New South Wales and the connection between the Sydney and Bowen Basins. J. geol. Soc. Aust. 16:697-710.

Runnegar, B.N. 1974. The geological framework of New England. In: C.G. Murray and B. Runnegar (Editors), Field Conference, New England Area. Geol. Soc. Aust., Queensl. Div. pp. 9-19.

Russell, T.G. and Middleton, M.F. 1981. Coal rank and organic diagenesis studies in the Gunnedah Basin: preliminary results. N.S.W. Geol. Surv., Q. Notes 45:1-11.

Rust, B.R. 1978. Depositional models for braided alluvium. In: A.D. Miall (Editor), Fluvial Sedimentology. Canadian Society of Petroleum Geologists, Alberta, Canada, pp. 605-625.

Rust, B.R. 1979. Facies models 2. Coarse alluvial deposits. In: R.G. Walker (Editor), Facies Models. Geological Association of Canada, pp. 9-21.

Schmincke, H-R. and Swanson, D.A. 1967. Laminar viscous flowage structures in ash-flow tuffs from Gran Canaria, Canary Islands. J. Geol. 75:641-664.

Schmincke, H-U., Fisher, R.V. and Waters, A.C. 1973. Antidune and chute and pool structures in the base surge deposits of the Laacher See area, Germany. Sedimentology 20:553-574.

Scholl, D.W., Christiansen, M.N., Von Huene, R. and Marlow, M.S. 1970. Peru-Chile trench sediments and sea-floor spreading. Bull. geol. Soc. Am. 81:1339-1360.

Self, S. 1983. Large-scale phreatomagmatic silicic volcanism: a case study from New Zealand. J. Volcanol. Geotherm. Res. 17:433-469.

Self, S. and Sparks, R.S.J. 1978. Characteristics of widespread pyroclastic deposits formed by the interaction of silicic magma and water. Bull. Volcanol. 41:196-212.

Self, S. and Wright, J.V. 1983. Large wave forms from the Fish Canyon Tuff, Colorado. Geology 11:443-446.

Self, S., Kienle, J. and Huot, J-P. 1980. Ukinrek Maars, Alaska, II. Deposits and formation of the 1977 craters. J. Volcanol. Geotherm. Res. 7:39-65.

Selley, R.C. 1970. Ancient Sedimentary Environments. Chapman and Hall Ltd., London, 237 pp.

Settle, M. 1978. Volcanic eruption clouds and the thermal power output of explosive eruptions. J. Volcanol. Geotherm. Res. 3: 309-324.

Shaw, S.E. 1969. Granitic rocks from the northern portion of the New England Batholith. In: G.H. Packham (Editor), The Geology of New South Wales. J. geol. Soc. Aust. 16:285-290.

Shaw, S.E. and Flood, R.H. 1981. The New England Batholith, eastern Australia: geochemical variation in time and space. J. geophys. Res. 86:10530-10544.

Shaw, S.E., Flood, R.H. and Vernon, R.H. 1982. Permian volcanism associated with the New England Batholith. In: F.L. Sutherland and J.R. Hardie (Editors), Symposium on Volcanism in Eastern Australia with Case Histories from N.S.W. Geol. Soc. Aust., Abstracts 7:7-8.

Shepherd, J.B. and Sigurdsson, H. 1982. Mechanism of the 1979 explosive eruption of Soufriere volcano, St. Vincent. J. Volcanol. Geotherm. Res. 13:119-130.

Sheridan, M.F. 1971. Particle-size characteristics of pyroclastic tuffs. J. geophys. Res. 76:5627-5634.

Sheridan, M.F. 1979. Emplacement of pyroclastic flows: a review. In: C.E. Chapin and W.E. Elston (Editors), Ash-flow Tuffs. Spec. Pap. geol. Soc. Am. 180:125-136.

Sheridan, M.F. 1980. Pyroclastic block flow from the September, 1976, eruption of La Soufrière volcano, Guadeloupe. Bull. Volcanol. 43:397-402.

Sheridan, M.F. and Updike, R.G. 1975. Sugarloaf Mountain tephra - a Pleistocene rhyolitic deposit of base-surge origin in northern Arizona. Bull. geol. Soc. Am. 86:571-581.

Sheridan, M.F. and Wohletz, K.H. 1981. Hydrovolcanic explosions: the systematics of water-pyroclast equilibration. Science 212: 1387-1389.

Sheridan, M.F. and Marshall, J.R. 1983. Interpretation of pyroclast surface features using SEM images. J. Volcanol. Geotherm. Res. 16:153-159.

Sheridan, M.F. and Wohletz, K.H. 1983a. Hydrovolcanism: basic considerations and review. J. Volcanol. Geotherm. Res. 17:1-29.

Sheridan, M.F. and Wohletz, K.H. 1983b. Origin of accretionary lapilli from the Pompeii and Avellino deposits of Vesuvius. In: R. Gooley (Editor), Microbeam Analysis - 1983. San Francisco Press Inc., San Francisco, pp. 35-38.

Sheridan, M.F., Barberi, F., Rosi, M. and Santacroce, R. 1981. A model for Plinian eruptions of Vesuvius. Nature 289:282-285.

Skilbeck, C.G. 1982. Carboniferous depositional systems of the Myall Lakes district, northern New South Wales. In: P.G. Flood and B. Runnegar (Editors), New England Geology. Department of Geology, University of New England and AHV Club, pp. 121-132.

Slack, J.F. and Lipman, P.W. 1979. Chronology of alteration, mineralization, and caldera evolution in the Lake City area, western San Juan Mountains, Colorado. In: J.D. Ridge (Editor), Papers on Mineral Deposits of Western North America, Fifth I.A.G.O.D. Symposium. Nevada Bureau Mines Geol., report 33:151-158.

Smith, A.L. and Roobol, M.J. 1982. Andesitic pyroclastic flows. In: R.S. Thorpe (Editor), Andesites. John Wiley and Sons, pp. 416-433.

Smith, A.L., Fisher, R.V., Roobol, M.J. and Wright, J.V. 1981. Pyroclastic flows and surges: examples from the Lesser Antilles. In: S. Self and R.S.J. Sparks (Editors), Tephra Studies. D. Reidel Publishing Company, pp. 421-425.

Smith, E.I. 1973. Mono Craters, California: a new interpretation of the eruption sequence. Bull. geol. Soc. Am. 84:2685-2690.

Smith, E.I. 1976. Structure and petrology of the John Kerr Peak dome complex, southwestern New Mexico. In: W.E. Elston and S.A. Northrop (Editors), Cenozoic Volcanism in Southwestern New Mexico. New Mex. geol. Soc., Spec. Publ. 5:71-78.

Smith, R.L. 1960a. Ash flows. Bull. geol. Soc. Am. 71:795-842.

Smith, R.L. 1960b. Zones and zonal variations of welded ash flows. Prof. Pap. U.S. geol. Surv. 354-F:149-159.

Smith, R.L. 1979. Ash-flow magmatism. In: C.E. Chapin and W.E. Elston (Editors), Ash-flow Tuffs. Spec. Pap. geol. Soc. Am. 180:5-27.

Smith, R.L. and Bailey, R.A. 1966. The Bandelier Tuff: a study of ash-flow eruption cycles from zoned magma chambers. Bull. Volcanol. 29:83-104.

Smith, R.L. and Bailey, R.A. 1968. Resurgent cauldrons. In: R.R. Coats and others (Editors), Studies in Volcanology. Mem. geol. Soc. Am. 116:613-662.

Smith, R.L., Bailey, R.A. and Ross, C.S. 1961. Structural evolution of the Valles caldera, New Mexico, and its bearing on the emplacement of ring dikes. Prof. Pap. U.S. geol. Surv. 424-D:145-149.

Sparks, R.S.J. 1975. Stratigraphy and geology of the ignimbrites of Vulsini Volcano, Central Italy. Geol. Rdsch. 64:497-523.

Sparks, R.S.J. 1976. Grain size variations in ignimbrites and implications for the transport of pyroclastic flows. Sedimentology 23:147-188.

Sparks, R.S.J. 1978a. Gas release rates from pyroclastic flows: an assessment of the role of fluidisation in their emplacement. Bull. Volcanol. 41:1-9.

Sparks, R.S.J. 1978b. The dynamics of bubble formation and growth in magmas: a review and analysis. J. Volcanol. Geotherm. Res. 3:1-37.

Sparks, R.S.J. and Walker, G.P.L. 1973. The ground surge deposit: a third type of pyroclastic rock. Nature 241:62-64.

Sparks, R.S.J. and Wilson, L. 1976. A model for the formation of ignimbrite by gravitational column collapse. J. geol. Soc. Lond. 132:441-451.

Sparks, R.S.J. and Walker, G.P.L. 1977. The significance of vitric-enriched air-fall ashes associated with crystal-enriched ignimbrites. J. Volcanol. Geotherm. Res. 2:329-341.

Sparks, R.S.J. and Huang, T.C. 1980. The volcanological significance of deep-sea ash layers associated with ignimbrites. Geol. Mag. 117:425-436.

Sparks, R.S.J., Self, S. and Walker, G.P.L. 1973. Products of ignimbrite eruptions. Geology 1:115-118.

Sparks, R.S.J., Wilson, L. and Hulme, G. 1978. Theoretical modeling of the generation, movement, and emplacement of pyroclastic flows by column collapse. J. geophys. Res. 83:1727-1739.

Sparks, R.S.J., Wilson, L. and Sigurdsson, H. 1981. The pyroclastic deposits of the 1875 eruption of Askja, Iceland. Philos. Trans. R. Soc. Lond. 299:241-273.

Steven, T.A. and Lipman, P.W. 1976. Calderas of the San Juan volcanic field, southwestern Colorado. Prof. Pap. U.S. geol. Surv. 958.

Steven, T.A., Luedke, R.G. and Lipman, P.W. 1974. Relation of mineralization to calderas in the San Juan volcanic field, southwestern Colorado. J. Res. U.S. geol. Surv. 2:405-409.

Stoertz, G.E. and Ericksen, G.E. 1974. Geology of salars in northern Chile. Prof. Pap. U.S. geol. Surv. 811.

Streckeisen, A. 1976. To each plutonic rock its proper name. Earth Sci. Rev. 12:1-33.

Tadros, N.Z. 1982. Geology and coal resources west of Boggabri. N.S.W. Geol. Surv., Q. Notes 48:2-14.

Thomson, J. 1976. Geology of the Drake 1:100 000 sheet 9340. Geol. Surv. N.S.W. 185 pp.

Thorpe, R.S., Francis, P.W. and Moorbath, S. 1979. Rare earth and strontium isotope evidence concerning the petrogenesis of North Chilean ignimbrites. Earth Planet. Sci. Lett. 42:359-367.

Thorpe, R.S., Francis, P.W., Hammill, M. and Baker, M.C.W. 1982. The Andes. In: R.S. Thorpe (Editor), Andesites. John Wiley and Sons, pp. 187-205.

Tunbridge, I.P. 1981. Sandy high-energy flood sedimentation - some criteria for recognition, with an example from the Devonian of S.W. England. Sediment. Geol. 28:79-85.

Tunbridge, I.P. 1983. Alluvial fan sedimentation of the Horseshoe Park Flood, Colorado, U.S.A., July 15th, 1982. Sediment. Geol. 36:15-23.

Vernon, R.H. 1983. Restite, xenoliths and microgranitoid enclaves in granites. J. Proc. R. Soc. N.S.W. 116:77-103.

Voisey, A.H. and Williams, K.L. 1964. The geology of the Carroll-Keepit-Rangari area of New South Wales. J. Proc. R. Soc. N.S.W. 97:65-72.

Vucetich, C.G. and Pullar, W.A. 1969. Stratigraphy and chronology of late Pleistocene volcanic ash beds in central North Island, New Zealand. N.Z. Jl. Geol. Geophys. 12:784-837.

Walker, G.P.L. 1971. Grain-size characteristics of pyroclastic deposits. J. Geol. 79:696-714.

Walker, G.P.L. 1972. Crystal concentration in ignimbrites. Contr. Mineral. Petrol. 36:135-146.

Walker, G.P.L. 1973a. Explosive volcanic eruptions - a new classification scheme. Geol. Rdsch. 62:431-446.

Walker, G.P.L. 1973b. Length of lava flows. Philos. Trans. R. Soc. Lond., Ser. A. 274:107-118.

Walker, G.P.L. 1979. A volcanic ash generated by explosions where ignimbrite entered the sea. Nature 281:642-646.

Walker, G.P.L. 1980. The Taupo Pumice: product of the most powerful known (ultraplinian) eruption? J. Volcanol. Geotherm. Res. 8:69-94.

Walker, G.P.L. 1981a. Characteristics of two phreatoplinian ashes, and their water-flushed origin. J. Volcanol. Geotherm. Res. 9: 395-407.

Walker, G.P.L. 1981b. The Waimihia and Hatepe plinian deposits from the rhyolitic Taupo Volcanic Centre. N.Z. Jl. Geol. Geophys. 24:305-324.

Walker, G.P.L. 1981c. Generation and dispersal of fine ash and dust by volcanic eruptions. J. Volcanol. Geotherm. Res. 11:81-92.

Walker, G.P.L. 1981d. Plinian eruptions and their products. Bull. Volcanol. 44:223-240.

Walker, G.P.L. 1981e. New Zealand case histories of pyroclastic studies. In: S. Self and R.S.J. Sparks (Editors), Tephra Studies. D. Reidel Publishing Company, pp. 317-330.

Walker, G.P.L. 1981f. Volcanological applications of pyroclastic studies. In: S. Self and R.S.J. Sparks (Editors), Tephra Studies. D. Reidel Publishing Company, pp. 391-403.

Walker, G.P.L. 1982. Eruptions of andesitic volcanoes. In: R.S. Thorpe (Editor), Andesites. John Wiley and Sons, pp. 403-413.

Walker, G.P.L. 1983. Ignimbrite types and ignimbrite problems. J. Volcanol. Geotherm. Res. 17:65-88.

Walker, G.P.L. 1984. Characteristics of dune-bedded pyroclastic surge bedsets. J. Volcanol. Geotherm. Res. 20:281-296.

Walker, G.P.L. and Croasdale, R. 1970. Two Plinian-type eruptions in the Azores. J. geol. Soc. Lond. 127:17-55.

Walker, G.P.L. and Croasdale, R. 1972. Characteristics of some basaltic pyroclastics. Bull. Volcanol. 35:303-317.

Walker, G.P.L. and McBroome, L.A. 1983. Mount St. Helens 1980 and Mount Pelée 1902 - flow or surge? Geology 11:571-574.

Walker, G.P.L. and Wilson, C.J.N. 1983. Lateral variations in the Taupo ignimbrite. J. Volcanol. Geotherm. Res. 18:117-133.

Walker, G.P.L., Heming, R.F. and Wilson, C.J.N. 1980a. Low-aspect ratio ignimbrites. Nature 283:286-287.

Walker, G.P.L., Heming, R.F. and Wilson, C.J.N. 1980b. Ignimbrite veneer deposits or pyroclastic surge deposits? Reply. Nature 286:912.

Walker, G.P.L., Wilson, C.J.N. and Froggatt, P.C. 1980. Fines-depleted ignimbrite in New Zealand - the product of a turbulent pyroclastic flow. Geology 8:245-249.

Walker, G.P.L., Self, S. and Froggatt, P.C. 1981. The ground layer of the Taupo ignimbrite: a striking example of sedimentation from a pyroclastic flow. J. Volcanol. Geotherm. Res. 10:1-11.

Walker, G.P.L., Wilson, C.J.N. and Froggatt, P.C. 1981. An ignimbrite veneer deposit: the trail-marker of a pyroclastic flow. J. Volcanol. Geotherm. Res. 9:409-421.

Walker, G.P.L., Heming, R.F., Sprod, T.J. and Walker, H.R. 1981. Latest major eruptions of Rabaul volcano. In: R.W. Johnson (Editor), Cooke-Ravian Volume of Volcanological Papers. Geological Survey of Papua New Guinea, Memoir 10:181-193.

Walker, G.P.L., Wright, J.V., Clough, B.J. and Booth, B. 1981. Pyroclastic geology of the rhyolitic volcano of La Primavera, Mexico. Geol. Rdsch. 70:1100-1118.

Walker, R.G. and Middleton, G.V. 1979. Facies models 4. Eolian Sands. In: R.G. Walker (Editor), Facies models. Geological Association of Canada, pp. 33-41.

Warner, D.S. 1972. Late Palaeozoic stratigraphy and sedimentation in the Murrurundi area, New South Wales. Unpub. B.Sc. (Hons) Thesis, University of New England, Armidale, 82 pp.

Waterhouse, J.B. 1978. Chronostratigraphy for the World Permian. In: Contributions to the Geologic Time Scale. AAPG Studies in Geology 6:299-322.

Waters, A.C. and Fisher, R.V. 1971. Base surges and their deposits: Capelinhos and Taal volcanoes. J. geophys. Res. 76:5596-5614.

Whetten, J.T. 1965. Carboniferous glacial rocks from the Werrie Basin, New South Wales, Australia. Bull. geol. Soc. Am. 76:43-56.

White, A.H. 1965. Geological Map of New England 1:100 000 Tareela Sheet (no. 300), with marginal text. University of New England, Armidale, N.S.W., Australia.

White, A.H. 1968. The glacial origin of Carboniferous conglomerates west of Barraba, New South Wales. Bull. geol. Soc. Am. 79:675-686.

Whitney, J.A. and Stormer, J.C. 1983. Igneous sulfides in the Fish Canyon Tuff and the role of sulfur in calc-alkaline magmas. Geology 11:99-102.

Wilkinson, J.F.G. 1971. The petrology of some vitrophyric calc-alkaline volcanics from the Carboniferous of New South Wales. J. Petrol. 12:587-619.

Wilkinson, J.F.G. and Whetten, J.T. 1964. Some analcime-bearing pyroclastic and sedimentary rocks from New South Wales. J. sediment. Petrol. 34:543-553.

Wilkinson, J.F.G., Vernon, R.H. and Shaw, S.E. 1964. The petrology of an adamellite-porphyrite from the New England Bathylith (New South Wales). J. Petrol. 5:461-488.

Williams, H. 1941. Calderas and their origin. Univ. Calif. Publ. Geol. Sci. 25:239-346.

Wilson, C.J.N. 1980. The role of fluidization in the emplacement of pyroclastic flows: an experimental approach. J. Volcanol. Geotherm. Res. 8:231-249.

Wilson, C.J.N. 1984. The role of fluidization in the emplacement of pyroclastic flows, 2: experimental results and their interpretation. J. Volcanol. Geotherm. Res. 20:55-84.

Wilson, C.J.N. and Walker, G.P.L. 1981. Violence in pyroclastic flow eruptions. In: S. Self and R.S.J. Sparks (Editors), Tephra Studies. D. Reidel Publishing Company, pp. 441-448.

Wilson, C.J.N. and Walker, G.P.L. 1982. Ignimbrite depositional facies: the anatomy of a pyroclastic flow. J. geol. Soc. Lond. 139:581-592.

Wilson, L. 1976. Explosive volcanic eruptions-III. Plinian eruption columns. Geophys. J. R. astr. Soc. 45:543-556.

Wilson, L., Sparks, R.S.J. and Walker, G.P.L. 1980. Explosive volcanic eruptions-IV. The control of magma properties and conduit geometry on eruption column behaviour. Geophys. J.R. astr. Soc. 63:117-148.

Wilson, L., Sparks, R.S.J., Huang, T.C. and Watkins, N.D. 1978. The control of volcanic column heights by eruption energetics and dynamics. J. geophys. Res. 83:1829-1836.

Winchester, J.A. and Floyd, P.A. 1977. Geochemical discrimination of different magma series and their differentiation products using immobile elements. Chem. Geol. 20:325-343.

Wohletz, K.H. 1983. Mechanisms of hydrovolcanic pyroclast formation: grain-size, scanning electron microscopy, and experimental studies. J. Volcanol. Geotherm. Res. 17:31-63.

Wohletz, K.H. and Sheridan, M.F. 1979. A model of pyroclastic surge. In: C.E. Chapin and W.E. Elston (Editors), Ash-flow Tuffs. Spec. Pap. geol. Soc. Am. 180:177-194.

Wohletz, K.H. and Sheridan, M.F. 1983. Hydrovolcanic explosions II. Evolution of basaltic tuff rings and tuff cones. Am. J. Sci. 283: 385-413.

Wolff, J.A. and Wright, J.V. 1981. Rheomorphism of welded tuffs. J. Volcanol. Geotherm. Res. 10:13-34.

Wood, B.L. 1982. The geology and mineralization of the Emmaville tin field. In: P.G. Flood and B. Runnegar (Editors), New England Geology. Department of Geology, University of New England and AHV Club, pp. 335-344.

Wood, C.A. 1974. Reconnaissance geophysics and geology of the Pinacate craters, Sonora, Mexico. Bull. Volcanol. 38:149-172.

Wright, J.V. 1981. The Rio Caliente Ignimbrite: analysis of a compound intraplinian ignimbrite from a major late Quaternary Mexican eruption. Bull. Volcanol. 44:189-212.

Wright, J.V. and Walker, G.P.L. 1977. The ignimbrite source problem: significance of a co-ignimbrite lag-fall deposit. Geology 5:729-732.

Wright, J.V. and Walker, G.P.L. 1981. Eruption, transport and deposition of ignimbrite: a case study from Mexico. J. Volcanol. Geotherm. Res. 9:111-131.

Wright, J.V., Smith, A.L. and Self, S. 1980. A working terminology of pyroclastic deposits. J. Volcanol. Geotherm. Res. 8:315-336.

Wright, J.V., Self, S. and Fisher, R.V. 1981. Towards a facies model for ignimbrite-forming eruptions. In: S. Self and R.S.J. Sparks (Editors), Tephra Studies. D. Reidel Publishing Company, pp. 433-439.

Wright, J.V., Roobol, M.J., Smith, A.L., Sparks, R.S.J., Brazier, S.A., Rose, W.I. and Sigurdsson, H. 1984. Late Quaternary explosive silicic volcanism on St Lucia, West Indes. Geol. Mag. 121:1-15.

Yokoyama, S. 1974. Mode of movement and emplacement of Ito pyroclastic flow from Aira Caldera, Japan. Sci. Rep. Tokyo Kyoiku Daigaku C12:17-62.

Yokoyama, S. 1981. Base surge deposits in Japan. In: S. Self and R.S.J. Sparks (Editors), Tephra Studies. D. Reidel Publishing Company, pp. 427-432.

APPENDIX A

DEXTRAL MOVEMENT ON THE DEMON FAULT, NORTHEASTERN NEW SOUTH WALES: A REASSESSMENT

J. McPHIE AND C.L. FERGUSSON[1]

Department of Geology and Geophysics, University of New England, Armidale, 2351.

[1]Present address: Department of Earth Sciences, Monash University, Clayton, 3168.

ABSTRACT. The Demon Fault is a meridional transcurrent fault extending for at least 200 km in the eastern part of the New England Orogen. The southern margin of the Late Permian Coombadjha Volcanic Complex, and contacts between units within it, are displaced for 23 km in a dextral sense along the Fault. In the Cooraldooral Creek area the Fault consists of at least four major fractures. This contrasts with the Timbarra River area where the trace of the Fault is marked by an elongate zone of sheared rock 500 m wide.

INTRODUCTION

The Demon Fault (or Fault System) was recognized by Shaw (1969) to be a major transcurrent fault in the New England Orogen of north-eastern New South Wales (Fig. A.1). The Fault extends from Ebor in the south for 200 km following a northward meridional trend. Shaw (1969, p.285) estimated dextral strike-slip movement amounting to about 30 km on the basis of the displacement of the Stanthorpe Adamellite.

Korsch *et al.* (1978) documented the general characteristics of the Demon Fault and described its effects in detail for two sites. They rejected Shaw's estimate in favour of offset totalling only 17 km. This result was obtained by matching the contact between the Dundee Rhyodacite and the Bungulla Porphyritic Adamellite on either side of the Fault in the Timbarra River area (Korsch *et al.*, 1978, Fig. 3).

Further fieldwork in the Timbarra River area, herein reported,

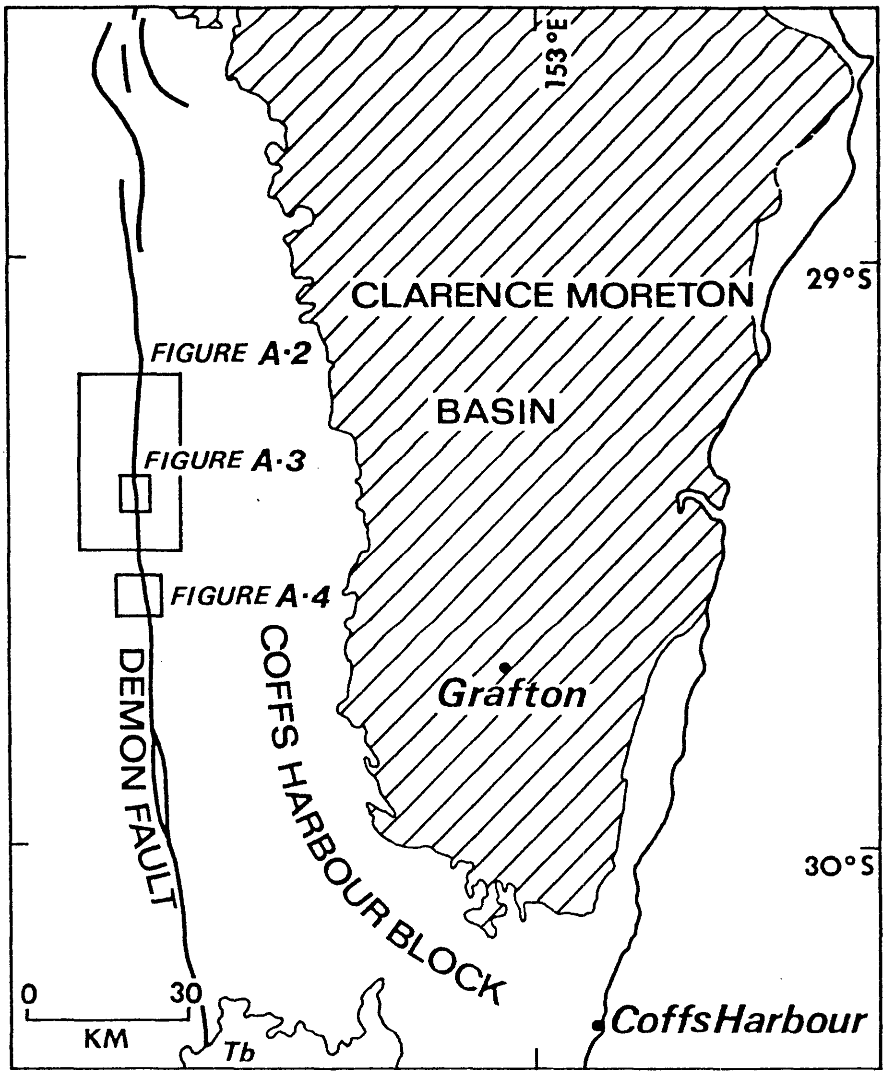

Figure A.1: Locality map for the areas discussed, northeastern New South Wales. Tb, Tertiary basalt.

indicates 23 km of dextral movement on the Demon Fault since the time of emplacement of the Early Triassic Dandahra Creek Granite. Details of the character of the Fault in this area and at one other locality (Cooraldooral Creek) are also described.

DISPLACEMENT OF THE COOMBADJHA VOLCANIC COMPLEX

The Coombadjha Volcanic Complex comprises Late Permian continental silicic volcanics and granitoids preserved adjacent and to the east of the Demon Fault in the upper reaches of Coombadjha and Washpool Creeks (Fig. A.2). The Complex has a mappable internal stratigraphy and structure which suggest that it is the eroded remnant of a volcanic cauldron (McPhie, 1982). Only those features relevant to the movement on the Demon Fault are described here.

Volcanic and plutonic rocks of the Complex that form its southern margin are intruded by the Dandahra Creek Granite, and all these rock units are truncated by the Demon Fault. Three of the five volcanic units of the Coombadjha Volcanic Complex can be traced to the Fault. The two older units (Pheasant Creek Volcanics and Pi Pi Ignimbrite, Chapter 6; Units A and C, McPhie, 1982) are both composed predominantly of outflow sheets of welded ignimbrite. In the field, these units are distinguishable from each other on the basis of the mineralogy and proportion of crystal fragments, and on the nature of the pumice lenticle foliation. The youngest unit is a representative of the Dundee Rhyodacite, a widespread and distinctive crystal-rich ignimbrite characterised by tor-like outcrops and textures similar to those of porphyritic granitoids. These three volcanic units dip to the north or northwest at shallow angles (10° to 25°). The contact with the Dandahra Creek Granite is sharp, and dips steeply to the north.

These same three volcanic units and the Dandahra Creek Granite have been located to the north on the west side of the Demon Fault (Fig. A.2). Contacts between the volcanic units, and between the volcanics and the Dandahra Creek Granite on the east side of the Fault are consistently offset for 23 km in a dextral sense to the Boundary Creek area. The quality of outcrop in this area west of the Fault is poorer, particularly within the Dundee Rhyodacite. Farther west, the Complex is intruded by the Billyrimba Leucoadamellite. To the north in the Demon Creek area, the Dundee Rhyodacite outcrops in isolated patches surrounded by microgranite that forms the shallowly east-dipping roof zone of the Bungulla Porphyritic Adamellite. In this area, no single, straight-line contact exists between the Dundee Rhyodacite and the Bungulla Porphyritic Adamellite (*cf.* Korsch *et al.*, 1978, Fig. 3).

THE DEMON FAULT IN THE TIMBARRA RIVER AREA

Here the Demon Fault separates the Coombadjha Volcanic Complex to the east from undifferentiated, complexly deformed Palaeozoic sedimentary rocks to the west (Fig. A.3). One main fracture is present, marked by poor exposure. For 500 m to the west of this fracture, the deformed Palaeozoic rocks are pervasively sheared with many randomly-oriented shear surfaces and complete destruction of sedimentary layering. The volcanics on the east side within 50 m of the fracture are closely jointed.

The complexly deformed rocks on the west consist of argillite, argillite-tuffaceous mudstone, massive tuffaceous(?) rock, thin-bedded turbidite and massive greywacke. Bedding in much of this sequence is near vertical and strikes northwest. Uncommon exposures of graded bedding and micro-crosslamination indicate northeasterly younging directions. Slaty cleavage is sporadically present in argillite.

THE DEMON FAULT IN THE COORALDOORAL CREEK AREA

There are two major arms of the Demon Fault in the Cooraldooral Creek area (Fig. A.4), each marked by prominent aerial photolineaments. These fault branches are entirely within complexly deformed sedimentary rocks. Two informal units of the Coffs Harbour beds occur east of the Fault (Fig. A.4): a northeastern unit (Chb_2) of argillite and less abundant thin-bedded turbidite and massive greywacke, and a southwestern unit (Chb_1) of thin-bedded turbidite and massive greywacke in similar proportions. To the west of the Fault, the sequence is dominated by argillite with less abundant thin-bedded turbidite, massive greywacke

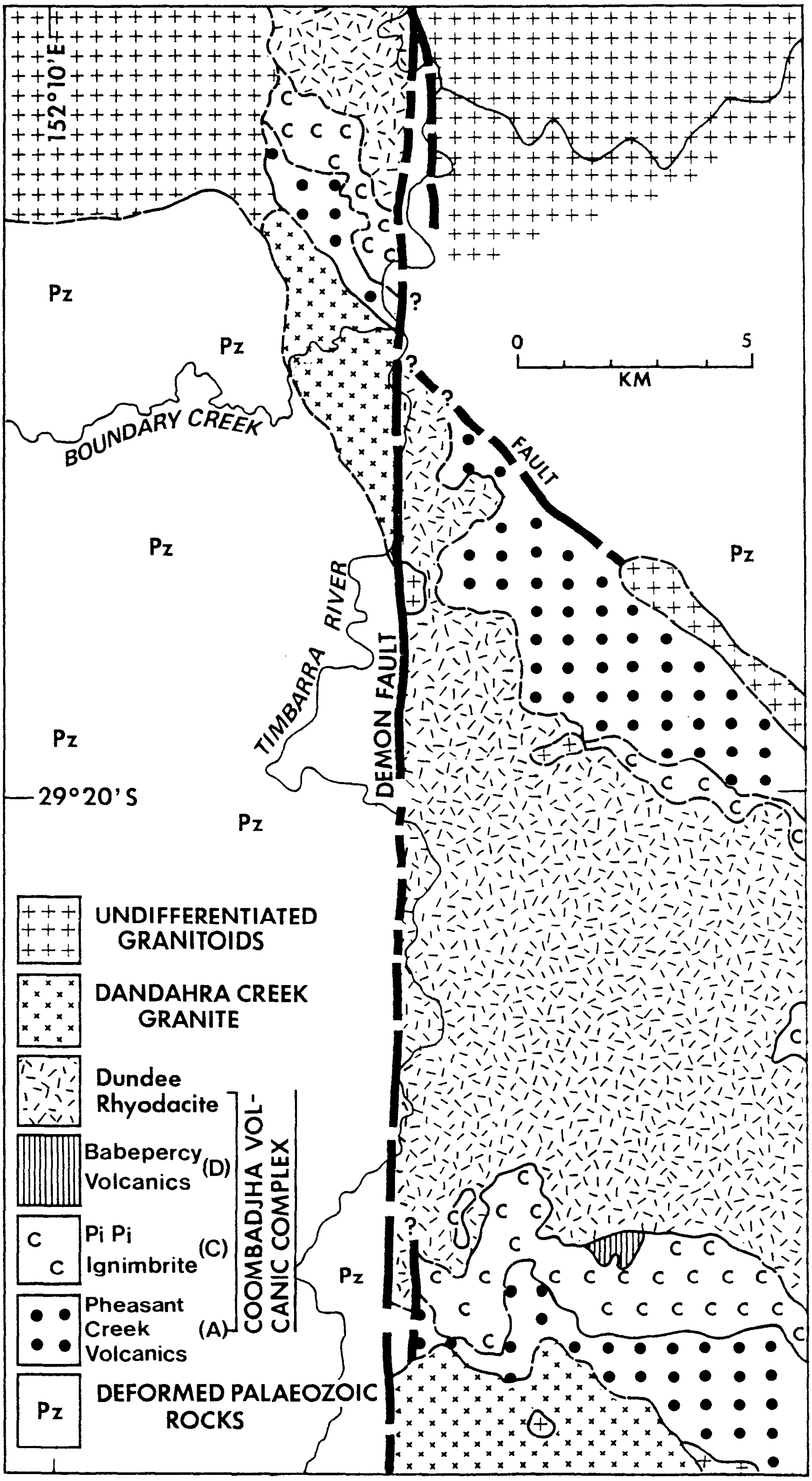

Figure A.2: The geology of the Timbarra River area showing the 23 km of dextral displacement of the Coombadjha Volcanic Complex along the Demon Fault.

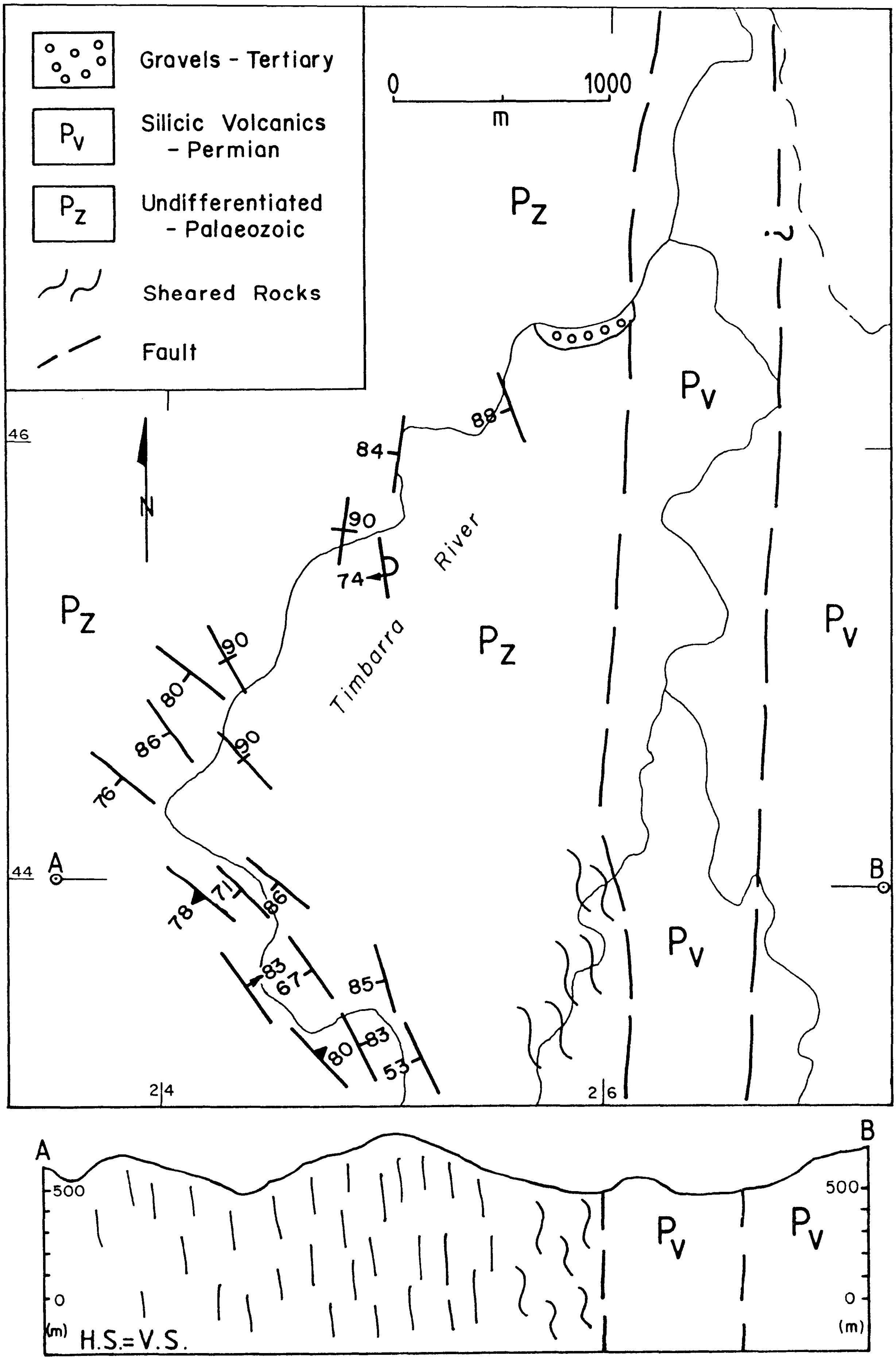

Figure A.3: Detailed map and cross-section of the Demon Fault along the Timbarra River. See Figure A.4 for a key to the structural symbols.

and intermediate volcanics. Areas of sheared rocks are exposed in Barool Creek 1 km west of the Fault. Bedding on both sides of the Fault is steeply dipping and northwesterly striking, with most younging directions facing towards the northeast. In the Coffs Harbour beds there are at least two tight to isoclinal folds pairs, with west-younging limbs up to 500 m across, and sporadically developed slaty cleavage in argillites.

Two additional fractures to the west of the main arms of the Fault offset an east-west trending, vertical, quartz-feldspar porphyry dyke (Fig. A.4). The dyke is up to 100 m in width and forms a cliff line, the displacement of which is readily apparent on aerial photographs.

CONCLUSIONS

Detailed mapping of silicic volcanics either side of the Demon Fault provides evidence for 23 km of dextral strike-slip movement. The relationships herein described confirm that this movement occurred after the cessation of Permo-Triassic silicic volcanic and intrusive activity within the region, as was implicit on Shaw's (1969, Fig. 4.9) map. Prior existence of the Fault is unlikely, since there is no indication of its influence on either the original stratigraphy or primary structure of the Coombadjha Volcanic Complex.

Study of the tectono-stratigraphic units of the Coffs Harbour Block has enabled correlation of this area with the Texas-Warwick area (Fergusson, 1982; Flood and Fergusson, 1982). Extrapolation of boundaries of the equivalent tectono-stratigraphic units of each of these areas gives a result consistent with the 23 km of movement determined in this study of the Fault.

ACKNOWLEDGEMENTS

We thank Peter Flood for helpful discussions and his review of the manuscript.

REFERENCES

Fergusson, C.L. 1982. An ancient accretionary terrain in eastern New England - evidence from the Coffs Harbour Block. In: P.G. Flood and B. Runnegar (Editors), New England Geology. Department of Geology, University of New England and AHV Club, pp.63-70.

Flood, P.G. and Fergusson, C.L. 1982. Tectono-stratigraphic units and structure of the Texas-Coffs Harbour region. In: P.G. Flood and B. Runnegar (Editors), New England Geology. Department of Geology, University of New England and AHV Club, pp.71-88.

Korsch, R.J., Archer, N.R. and McConachy, G.W. 1978. The Demon Fault. J. Proc. R. Soc. N.S.W., 111:101-106.

McPhie, J. 1982. The Coombadjha Volcanic Complex: a Late Permian cauldron, northeastern New South Wales. In: P.G. Flood and B. Runnegar (Editors), New England Geology. Department of Geology, University of New England and AHV Club, pp.221-227.

Shaw, S.E. 1969. Granitic rocks from the northern portion of the New England Batholith. In: G.H. Packham (Editor), The Geology of New South Wales. J. geol. Soc. Aust., 16:285-290.

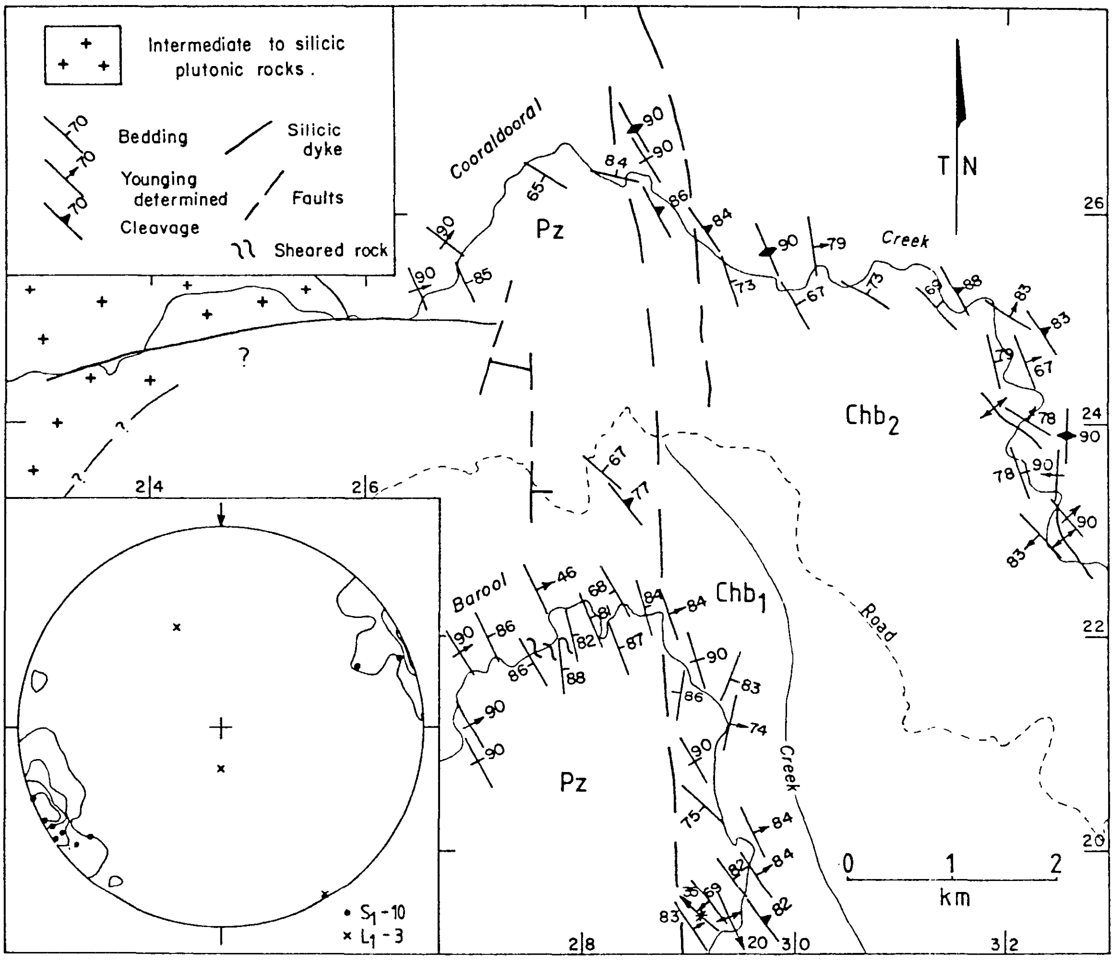

Figure A.4: Detailed map of the Demon Fault in the Cooraldooral Creek area. Equal-area stereographic projection of 58 poles to bedding contoured at 5,10,15,20% per 1% area.

Pz - undifferentiated Palaeozoic sedimentary rocks.

Chb_1, Chb_2, subunits of the Coffs Harbour beds.

APPENDIX B

MODAL DATA

The tables give modal analyses obtained by point counting thin-sections using a Swift Automatic Point Counter (mechanical stage, digital counting unit). The data have been presented on figures in the text as indicated below.

Chapter 2: Table B.1.

Chapter 3: Tables B.1, B.2.

Chapter 6: Tables B.3, B.5, B.6, B.9.

Chapter 7: Table B.4.

Chapter 8: Tables B.6, B.7, B.8.

TABLE B.1: Modes[1] of representative samples of ignimbrite members of the Currabubula Formation.

	Cana Creek Tuff Member			Iventure Ignimbrite Member			Taggarts Mountain Ignimbrite Member			Piallaway Trig Ignimbrite Member		
	R55049	R55045	R55104	R55155	R55148	R55149	R55206	R55212	R55213	R55274	R55276	R55278
Quartz	4	2	3	6	6	7	16	18	17	4	4	2
Total feldspar	4	5	4	14	14	10	28	24	29	20	23	22
Biotite	-	-	-	-	-	-	2	2	4	3	1	2
Opaque	-	-	-	tr[2]	tr	tr	tr	tr	1	1	1	1
Σ Crystals	8	7	7	20	20	17	46	44	51	28	29	27
Matrix	92	93	93	80	80	82	54	56	49	72	70	73
Lithic	tr	tr	tr	tr	tr	1	tr	tr	-	tr	1	tr

[1] 1000 points counted per thin-section, expressed as percentage points.

[2] Trace amount present.

TABLE B.2: Modes[1] of sandstones of the Cana Creek Tuff Member of the Currabubula Formation.

	R55090	R55093	R55094	R55101	R55121	R55128
Crystals	24.9	25.4	39.2	40.2	31.4	22.2
Vitric[2]	74.1	73.6	57.8	54.6	67.4	76.8
Lithic	1.0	1.0	3.0	5.2	1.2	1.0

[1] 1000 points counted per thin-section, expressed as percentage points.

[2] Includes pumice, shards and unresolvable fine grained matrix.

TABLE B.3: Modes[1] of ignimbrites of the Pheasant Creek Volcanics, Coombadjha Volcanic Complex.

	R55369	R55370	R55371	R55373	R55374	R55375	R55377	R55378	R55380	R55381	R55382	R55383	R55385	R55386	R55387	R55388	R55389	R55391	R55394	R55402
Quartz	1.5	1.3	0.8	2.0	1.2	1.1	0.8	1.3	0.9	0.8	3.9	2.3	0.4	tr[4]	4.3	0.6	2.8	3.1	3.2	-
Total feldspar	39.5	22.6	27.8	27.3	36.5	34.3	25.4	36.9	21.5	33.3	25.2	24.2	32.5	35.7	22.7	35.5	36.9	5.1	10.7	11.8
K-feldspar	u[3]	u	u	u	u	u	6.6	11.7	4.6	7.7	12.4	u	16.3	9.9	13.1	11.3	15.2	4.3	4.5	-
Biotite	0.7	1.9	0.7	0.4	0.5	1.3	3.3	2.2	2.2	3.0	2.0	3.1	1.6	4.1	1.6	3.7	2.0	-	-	-
Ferromagnesian[2]	2.3	0.6	1.7	1.2	1.3	2.1	0.8	0.9	0.8	2.3	1.4	0.8	3.0	2.7	0.2	1.2	0.4	0.3	2.0	0.4
Opaque	0.1	0.2	0.2	0.8	0.1	0.3	0.4	0.1	0.9	0.3	1.2	1.0	0.2	0.5	0.4	0.3	-	0.1	1.4	0.1
Σ Crystals	44.1	26.6	31.2	31.7	39.6	39.1	30.7	41.4	26.3	39.7	33.7	31.4	37.7	43.0	29.2	41.3	42.1	8.6	17.3	12.3
Matrix	55.9	73.4	68.8	66.5	60.4	60.9	69.3	58.6	73.7	60.0	66.3	68.6	61.3	55.6	70.8	58.7	57.9	91.4	82.7	87.7
Lithic	-	-	-	1.8	-	-	-	-	-	0.3	-	tr	1.0	1.4	-	-	-	-	-	-

[1] 1000 points counted per thin-section, expressed as percentage points.

[2] Extensively altered ferromagnesian mineral phase.

[3] Not differentiated from total feldspar count.

[4] Trace amount present.

TABLE B.4: Modes[1] of the massive porphyry facies of the Hianana Volcanics, Coombadjha Volcanic Complex.

	R55421	R55424	R55425	R55428	R55429	R55430
Feldspar	19.7	20.3	20.8	28.3	25.5	25.3
Ferromagnesian[2]	1.8	4.4	1.6	2.0	2.2	2.4
Opaque[3]	1.9	1.4	1.3	1.0	0.4	0.5
Σ Phenocrysts	23.4	26.1	23.7	31.3	28.1	28.2
Groundmass	76.6	73.9	76.3	68.7	71.9	71.8

[1] 1000 points counted per thin-section, expressed as percentage points.

[2] Extensively altered pyroxene and hornblende.

[3] Opaque phase is predominantly pyrite and is not necessarily primary.

TABLE B.5: Modes[1] of Pi Pi Ignimbrite, Coombadjha Volcanic Complex.

	R55432	R55433	R55435	R55436	R55438	R55439	R55440	R55441	R55442	R55443	R55445
Total feldspar	16.2	22.5	13.4	17.4	22.0	22.2	22.2	16.8	18.5	15.0	17.1
Ferromagnesian[2]	1.8	2.6	2.2	1.2	3.1	1.6	1.5	3.0	1.4	2.4	2.7
Opaque	0.3	0.8	0.3	0.3	0.4	0.6	0.3	0.9	0.7	-	-
Σ Crystals	18.3	25.9	15.9	18.9	25.5	24.4	24.0	20.7	20.6	17.4	19.8
Matrix	81.7	73.6	84.1	81.1	74.5	75.6	76.0	79.3	79.4	82.6	80.2
Lithic	-	0.5	-	-	-	-	-	-	-	-	-

[1] 1000 points counted per thin-section, expressed as percentage points.

[2] Extensively altered ferromagnesian phase.

TABLE B.6: Modes[1] of the Normal facies ignimbrite of the Dundee Rhyodacite.

	COOMBADJHA VOLCANIC COMPLEX													
	R55453	R55454	R55457	R55459	R55464	R55465	R55466	R55468	R55469	R55472	R55473	R55474	R55475	R55477
Quartz	7.8	6.9	10.2	6.7	4.7	6.2	6.0	2.8	4.1	6.8	4.6	2.9	7.4	2.2
Total feldspar	39.3	33.9	34.5	34.0	39.7	34.6	38.4	42.0	36.4	38.9	35.1	34.2	36.7	30.3
Biotite	9.7	10.3	10.1	13.1	11.4	11.8	14.0	10.1	9.3	9.7	7.2	10.4	10.8	9.5
Hornblende	4.1	3.1	3.0	3.6	3.3	2.6	3.0	6.3	2.5	3.7	4.4	3.8	3.7	4.2
Pyroxene	2.5	2.4	1.3	2.0	1.3	2.8	3.5	0.2	2.2	2.5	4.2	3.3	2.3	1.1
Opaque	1.2	1.0	0.7	0.7	0.4	0.4	1.2	0.3	0.6	0.8	0.4	1.0	0.8	0.4
Σ Crystals	64.6	57.6	59.8	60.1	60.8	58.4	66.1	61.7	55.1	62.4	55.9	55.6	61.7	47.7
Matrix	35.1	42.2	37.5	39.1	39.0	41.2	33.4	37.7	43.4	36.6	44.1	44.3	38.3	52.0
Inclusions	0.3	0.2	2.7	0.8	0.2	0.4	0.5	0.6	1.5	1.0	-	0.1	-	0.3

[1] 1000 points counted per thin-section, expressed as percentage points.

TABLE B.6: Modes[1] of the Dundee Rhyodacite continued.

	COOMBADJHA VOLCANIC COMPLEX								BRASSINGTON	TENTERFIELD		TARBAN		DUNDEE
	R55479	R55480	R55481	R55487	R55488	R55489	R55497[2]	R55501[2]	R55610	R55611	R55613	R55615	R55616	R55617
Quartz	7.0	2.6	8.5	3.7	6.4	5.3	4.8	5.0	2.1	6.7	6.7	5.3	2.8	4.8
Total feldspar	40.4	34.7	34.0	38.4	36.7	37.0	31.7	36.2	34.1	37.6	38.9	27.8	32.7	40.8
Biotite	10.4	8.6	8.9	11.9	8.5	9.3	8.6	10.6	9.0	9.6	10.4	6.1	10.0	6.8
Hornblende	3.2	3.4	2.5	4.1	3.6	1.6	4.5	2.5	2.9	2.7	2.3	2.8	3.0	2.8
Pyroxene	1.7	1.9	2.3	2.6	3.5	3.9	1.8	2.3	4.1	2.1	1.4	1.5	2.5	2.9
Opaque	0.5	1.1	1.2	1.2	1.8	1.0	0.9	0.4	0.8	1.0	0.6	0.5	0.5	0.9
Σ Crystals	63.2	52.3	57.4	61.9	60.5	58.1	52.3	57.0	53.0	59.7	60.3	44.0	51.5	59.0
Matrix	36.2	45.4	42.2	37.5	39.0	40.5	46.4	41.7	47.0	40.3	38.1	54.7	47.7	39.7
Inclusions	0.6	2.3	0.4	0.6	0.5	1.4	1.3	1.3	-	-	1.6	1.3	0.8	1.3

[1] 1000 points counted per thin-section, expressed as percentage points.

[2] Basal facies ignimbrite.

TABLE B.7: Modes[1] of lenticles (relic pumice) in Dundee Rhyodacite ignimbrite.

	Coombadjha Volcanic Complex			Brassington	Tenterfield	
	R55465	R55465	R55469	R55610	R55611	R55612
Quartz	4.2	14.0	1.2	1.5	0.8	4.4
Total feldspar	29.0	25.3	35.9	12.0	19.9	24.6
Biotite	9.4	5.7	6.5	3.7	6.4	4.2
Hornblende	1.4	0.8	2.3	0.8	0.4	1.3
Pyroxene	0.8	0.3	1.2	0.8	2.4	0.8
Opaque	0.6	0.3	0.4	0.8	0.8	0.2
Σ Phenocrysts	45.4	46.4	47.5	19.6	30.7	35.5
Groundmass	54.6	53.6	52.5	80.4	67.7	61.8
Inclusions	-	-	-	-	1.6	2.7
Points counted	500	384	259	133	251	476

[1] Expressed as percentage points.

TABLE B.8: Modes[1] of the porphyritic dacite of the Basal facies Dundee Rhyodacite, Coombadjha Volcanic Complex.

	R55506	R55509	R55514	R55515
Quartz	3.2	0.9	4.2	1.0
Total feldspar	31.0	30.2	25.2	21.3
Biotite	5.6	5.3	5.4	7.0
Hornblende	-	1.6	0.8	tr[3]
Pyroxene	2.8[2]	1.4	6.0[2]	2.0
Opaque	0.3	0.3	0.4	0.3
Σ Phenocrysts	42.9	39.7	42.0	31.6
Groundmass	55.1	60.0	58.0	67.0
Inclusions	2.0	0.3	-	1.4

[1] 1000 points counted per thin-section, expressed as percentage points.

[2] Extensively altered.

[3] Trace amount present.

TABLE B.9: Modes[1] of the Moonta Gully Adamellite of the Coombadjha Volcanic Complex.

	R55554	R55556	R55562
Quartz	23.8	20.4	20.8
Plagioclase	39.8	35.4	36.6
K-feldspar	22.4	28.8	28.4
Biotite	11.0	9.2	9.4
Hornblende	3.0	6.2	4.8

[1] 1000 points counted per thin-section, expressed as percentage points.

APPENDIX C

ANALYTICAL METHODS

Samples collected for major and trace element analyses were crushed to -200 mesh in a tungsten-carbide vessel of a Siebtechnik mill. Major elements other than sodium and ferrous iron were determined by X-ray fluorescence spectrometry (XRF) at the School of Earth Sciences, Macquarie University, Sydney, (analyst John Bedford) using the method of Norrish and Chappell (1977). Na_2O was determined by flame photometry and ferrous iron by titrometric methods, also at the School of Earth Sciences, Macquarie University. Trace element analyses were performed by X-ray fluorescence spectrometry in several runs using the appropriate tubes, at the School of Earth Sciences, Macquarie University (analyst John Bedford) following the procedures outlined by Norrish and Chappell (1977). Mass absorptions were calculated from the major element analyses.

Total H_2O was determined by weighing the cooled condensate collected after heating the powdered sample at 1050°C for one hour. H_2O^- was determined by measuring the loss in weight after heating the powdered sample at 100°C for one hour. H_2O^+ is reported as the difference between total H_2O and H_2O^-. Where necessary, CO_2 was measured using a Collins' Calcimeter apparatus.

REFERENCE

Norrish, K. and Chappell, B.W. 1977. X-ray fluorescence spectrometry. In: J. Zussman (Editor), Physical Methods in Determinative Mineralogy, Second Edition. Academic Press, London, pp.201-272.

APPENDIX D

LIST OF HANDSPECIMENS AND THIN-SECTIONS

List of hand specimens and thin-sections, Department of Geology and Geophysics, University of New England catalogue.

Abbreviations and symbols:
- loc. - personal mapping locality numbers
- PTIM - Piallaway Trig Ignimbrite Member
- TMIM - Taggarts Mountain Ignimbrite Member
- IIM - Iventure Ignimbrite Member
- * - chemical analysis
- M - modal analysis
- † - K-Ar date

The first half of each grid reference refers to 'eastings', and the second half refers to 'northings'.

R55021 to R55362: six-figure grid reference to the 1000 yard grid on Standard 2 inches to 1 mile Topographic Maps, New South Wales Department of Lands, Sydney.

Therribri	8936-IV-N						
Boggabri	8936-IV-S	Willuri	8936-I-S				
		Kelvin	8936-II-N				
		Gunnedah	8936-II-S	Somerton	9036-III-S		
				Winton	9035-IV-N		
				Piallaway	9035-IV-S		
				Werris Creek	9035-III-N	Goonoo Goonoo	9035-II-N
				Quipolly	9035-III-S	Emblem	9035-II-S
				Quirindi-A	9034-IV-N	Quirindi-B	350-B
						Quirindi-D	350-D

R55369 to R55614: eight-figure grid reference to 1000 metre Australian Map Grid on 1:25000 Series Topographic Maps, New South Wales Department of Lands, Sydney.

Tenterfield	9339-IV-N		
Sandy Flat	9339-IV-S	Malara Creek	9339-I-S
Spirabo	9339-III-N	Washpool	9339-II-N
Rockadooie	9339-III-S	Coombadjha	9339-II-S

R55615 and R55616: grid reference to 1000 metre Australian Map Grid 1:100 000 Series R631 Topographic Map, Sheet 9240, Stanthorpe, Department of Lands, New South Wales.

R55617: grid reference to 1000 metre Australian Map Grid on 1:100 000 Series R651 Topographic Map, Sheet 9239, Clive, New South Wales Department of Lands.

loc.	Catalogue number	Hand specimen	Thin-section	Map sheet and grid reference		Lithology
						Currabubula Formation Cana Creek Tuff Member
W16a	R55021	+	+	Winton	579496	Ignimbrite
W16b	R55022	+			579496	Ash-fall tuff
W22	R55023	+	+		575487	Ignimbrite
W53	R55024	+	+		626493	Ignimbrite
W53	R55025	+			626493	Ignimbrite
W59	R55026	+			625496	Ignimbrite
W91a	R55027	+			579509	Ignimbrite
W91b	R55028	+			579509	Ignimbrite
W99a	R55029	+	+		576506	Ignimbrite
W99b	R55030	+			576506	Ignimbrite
W99c	R55031	+			576506	Ash-fall tuff
W140	R55032	+			597534	Ignimbrite
W140	R55033	+			597534	Ash-fall tuff
W153	R55034	+			623500	Ignimbrite
W180A	R55035	+			567529	Ignimbrite
W180B	R55036	+	+		567529	Ignimbrite
W180C	R55037	+	+		567529	Ignimbrite
W180D	R55038	+	+		567529	Ash-fall tuff
W180E	R55039	+	+		567529	Ignimbrite
W180F	R55040	+			567529	Sandstone
W180G	R55041	+	+		567529	Ignimbrite
W180a	R55042	+	+		567529	Ignimbrite
W180b	R55043	+			567529	Ignimbrite
W180c	R55044	+			567529	Ignimbrite
W186	R55045*	+	+ M		576510	Ignimbrite
W188	R55046	+			565523	Ash-fall tuff
W534	R55047	+	+		564528	Ignimbrite
W31	R55048	+	+	Piall-	584470	Ash-fall tuff
W44a	R55049	+	+ M	away	590460	Ignimbrite
W44b	R55050	+			590460	Ignimbrite
W44B	R55051	+			590460	Sandstone
W44B'	R55052	+			590460	Ash-fall tuff
W73a	R55053	+	+		578481	Ignimbrite
W73b	R55054	+			578481	Ignimbrite
W73c	R55055	+	+		578481	Ignimbrite
W73d	R55056	+	+		578481	Accretionary lapilli tuff
W73g	R55057	+	+		578481	Ignimbrite
W73L	R55058	+			578481	Ash-fall tuff
W73D	R55059	+			578481	Ash-fall tuff
W102	R55060	+	+		584470	Sandstone
W102A	R55061	+	+		584470	Ignimbrite
W102B	R55062	+	+		584470	Ignimbrite
W102C	R55063	+	+		584470	Ignimbrite
W102D	R55064	+	+		584470	Ash-fall tuff
W102D	R55065	+	+		584470	Ash-fall tuff
W102E	R55066	+			584470	Granule conglomerate
W102a	R55067	+	+		584470	Ignimbrite
W102b	R55068	+			584470	Ash-fall tuff

loc.	Catalogue number	Hand specimen	Thin-section	Map sheet and grid reference		Lithology
W115	R55069	+	+	Piallaway	631483	Ignimbrite
W215	R55070	+	+		641449	Ignimbrite
W215	R55071	+	+		641449	Fine ash tuff
W227	R55072	+	+		649435	Fine ash tuff
W227a	R55073	+	+		649435	Ignimbrite
W234	R55074	+			639463	Ash-fall tuff
W253	R55075	+			644446	Accretionary lapilli tuff
W254	R55076	+			648445	Sandstone
W255	R55077	+	+		646441	Ignimbrite
W256	R55078	+	+		649435	Ignimbrite
W259a	R55079	+			666417	Fine ash tuff
W278	R55080	+	+		699362	Ignimbrite
W321	R55081	+			590452	Ash-fall tuff
W322	R55082	+			592448	Ignimbrite
W409	R55083	+			704360	Sandstone
W410	R55084	+	+		703358	Ignimbrite
W410a	R55085	+	+		703358	Ignimbrite
W421	R55086	+			711342	Ignimbrite
W421a	R55087	+	+		711342	Ignimbrite
W421b	R55088	+	+		711342	Ignimbrite
W446	R55089	+	+		706349	Ignimbrite
Q 2	R55090	+	+ M	Werris Ck.	740186	Sandstone
Q 14	R55091	+	+		726228	Coarse ash tuff
Q 14a	R55092	+			726228	Ignimbrite
Q 18	R55093	+	+ M		740245	Sandstone
Q 18	R55094	+	+ M		740245	Sandstone
Q 18a	R55095	+	+		740245	Ignimbrite
Q 60	R55096	+	+		725225	Ignimbrite
Q102	R55097*	+	+		738251	Ignimbrite
Q103	R55098	+	+		738256	Ignimbrite
Q302	R55099	+	+		737308	Sandstone
Q223	R55100*	+			557261	Ignimbrite
Q223A	R55101	+	+ M		557261	Sandstone
Q223B	R55102	+	+		557261	Ignimbrite
Q223C	R55103	+	+		557261	Ignimbrite
Q223D	R55104*	+	+ M		557261	Ignimbrite
Q223E	R55105	+	+		557261	Ash-fall tuff
Q223F	R55106	+	+		557261	Ash-fall tuff
Q223G	R55107	+	+		557261	Accretionary lapilli tuff
Q223H	R55108	+	+		557261	Ignimbrite
Q223I	R55109	+	+		557261	Ignimbrite
Q224	R55110	+	+		558265	Ignimbrite
Q 44	R55112	+	+	Quipolly	736146	Fine ash tuff
Q 45	R55113	+	+		738149	Ignimbrite
Q 45a	R55114	+	+		738149	Ignimbrite
Q 45b	R55115	+	+		738149	Ignimbrite
Q 45c	R55116	+	+		738149	Ignimbrite
Q 45D	R55117	+			738149	Ignimbrite
Q 45A	R55118	+	+		738149	Ignimbrite
Q 45e	R55119*				738149	Fine ash tuff
Q 3	R55120	+		Goonoo Goonoo	745186	Sandstone

loc.	Catalogue number	Hand specimen	Thin-section	Map sheet and grid reference		Lithology
Q 53	R55121	+	+ M	Emblem	742183	Sandstone
Q 54	R55122	+	+		743174	Sandstone
Q 62	R55123	+	+		743161	Ignimbrite
Q 62	R55124	+	+		743161	Ignimbrite
Q 63	R55125	+	+		743158	Ignimbrite
Q 66	R55126	+			742135	Ignimbrite
Q 66a	R55127	+			742135	Ignimbrite
Q 78	R55128	+	+ M		759112	Sandstone
Q 78a	R55129	+	+		759112	Ignimbrite
Q 79	R55130	+	+		758115	Ignimbrite
Q 79a	R55131	+			758115	Ignimbrite
Q 85	R55132	+	+		763091	Ignimbrite
Q 86	R55133	+	+		768086	Ignimbrite
Q 87	R55134	+	+		772081	Ignimbrite
Q310a	R55135	+			744132	Sandstone
Q310b	R55136	+			744132	Sandstone
Q310c	R55137	+	+		744132	Ignimbrite
Q310d	R55138	+	+		744132	Ignimbrite
Q322a	R55139	+	+		770060	Ignimbrite
PMT	R55140	+	+		773067	Ignimbrite
Q 91	R55141	+	+	Quirindi-B	781013	Ignimbrite
						<u>Iventure Ignimbrite Member</u>
W 9a	R55146	+	+	Winton	578534	
W148	R55147	+	+		598523	
W161	R55148	+	+ M		610508	
W163	R55149	+	+ M		578514	
W173	R55150	+	+		619497	
W458	R55151	+	+		507629	
W459	R55152	+	+		516629	
W459	R55153	+	+		516629	
W104	R55154*	+	+	Piallaway	586476	
W104	R55155	+	+ M		586476	
W191	R55156*	+	+		583482	
W191a	R55157*	+			583482	
W265	R55158	+	+		632466	
W390	R55159	+	+		645429	
Q 38	R55160	+	+	Quipolly	731170	
Q 50	R55161	+	+		732173	
Q 50	R55162	+	+		732173	
Q 50a	R55163	+	+		732173	
Q114	R55164	+	+		729181	
K138	R55165	+	+	Gunnedah	364749	
K 11	R55166	+	+	Willuri	312962	
K 41	R55167	+	+		289982	
K 53	R55168	+	+		303986	
						<u>Ignimbrite X</u> (Figs.2.2,2.4)
W 17	R55171	+	+	Winton	588497	
W 20	R55172	+	+		586488	
W 82	R55173	+	+		586491	
W190	R55174	+	+		584504	
W352	R55175	+	+		605511	
W352a	R55176	+	+		605511	

loc.	Catalogue number	Hand specimen	Thin-section	Map sheet and grid reference		Lithology
W379	R55177	+	+	Winton	589534	Member X continued
W431	R55178	+	+		615497	
W443	R55179	+	+		617496	
W203	R55180	+	+	Piallaway	636450	
W203	R55181	+	+		636450	
W435	R55182	+	+		585485	
W436	R55183	+	+		587477	
Q 70	R55184	+	+	Quipolly	727153	
Q 71	R55185	+	+		730159	
						Taggarts Mountain Ignimbrite Member
W 55c	R55187	+	+	Winton	622492	
W 83	R55188	+	+		588494	
W174a	R55189	+	+		621494	
W174b	R55190	+	+		621494	
W267	R55191	+	+		613499	
W304	R55192	+	+		591529	
W354	R55193	+	+		591526	
W373	R55194	+	+		608507	
W377a	R55195	+	+		592519	
W429	R55196	+	+		619492	
W466	R55197	+	+		498612	
W466	R55198*	+	+		498612	
W202	R55199	+	+	Piallaway	635446	
W210	R55200	+	+		636435	
W236	R55201	+	+		632452	
W385	R55202	+	+		642422	
W386	R55203	+	+		643429	
W434	R55204	+	+		586486	
W436a	R55205	+	+		642429	
W492	R55206	+	+ M		580421	
W492a	R55207	+	+		580421	
Q259a	R55210	+		Werris Ck.	576226	
Q268	R55211	+	+	Quipolly	569171	
Q287	R55212	+	+ M		571179	
Q416	R55213*	+	+ M		568179	
Q226	R55214*	+	+	Werris Ck.	562267	
Q227	R55215	+	+		548288	
Q243	R55216	+	+		576241	
Q245	R55217	+	+		566245	
Q349a	R55218*	+			569228	
Q349b	R55219	+	+		569228	
Q377a	R55220	+	+		572187	
Q413	R55221*	+	+		567198	
K112	R55222	+	+	Gunnedah	335758	
K130	R55223	+	+		344749	
K131	R55224	+	+		346751	
K136	R55225	+	+		358755	
K 71	R55226	+	+	Kelvin	283914	
K 90	R55227	+	+		278902	
K 97	R55228	+	+		294884	
K100	R55229	+	+		294874	

loc.	Catalogue number	Hand specimen	Thin-section	Map sheet and grid reference		Lithology
K153	R55230	+	+	Kelvin	314795	Taggarts Mt.Ig.Mbr.contd.
K155b	R55231	+	+		320798	
K160a	R55232	+	+		332794	
K179	R55233	+	+		278917	
K180	R55234	+			278915	
K181a	R55235	+	+		286919	
K 23	R55236	+	+	Willuri	284966	
K 26	R55237	+	+		273957	
K 39	R55238	+	+		286987	
R127	R55239	+	+		285032	
						Taggarts Mountain Ignimbrite Member vitrophyres
Q244a	R55240*	+	+	Werris Ck.	571245	
Q244d	R55241*	+			571245	
Q246a	R55242*	+	+		563246	
Q349	R55243	+	+		569228	
Q367a	R55244*	+	+		554278	
Q287a	R55245*	+	+	Quipolly	572179	
						Taggarts Mountain Ignimbrite textural variants
Q244b	R55246	+	+	Werris Ck.	571245	
Q244c	R55247	+	+		571245	
Q348a	R55248	+	+		575231	
Q367b	R55249	+	+		554278	
Q267	R55250	+	+	Quipolly	569171	
Q267a	R55251	+	+		569171	
Q288	R55252	+	+		565176	
Q385	R55253	+	+		572158	
Q392	R55254	+	+		566157	
K111	R55255	+		Gunnedah	333756	
K113a	R55256	+	+		338757	
K114	R55257	+	+		344757	
K126	R55258	+	+		327786	
K 92	R55259	+	+	Kelvin	282902	
K156	R55260	+	+		322797	
K174	R55261	+	+		323790	
K 2	R55262	+	+	Willuri	284974	
K 3	R55263	+	+		288965	
K 6	R55264	+	+		290957	
R131	R55265	+	+	Billyena	145354	Plagyan Rhyolite
R135	R55266	+	+		160360	
						Piallaway Trig Ignimbrite Member
W 19	R55267	+	+	Winton	591486	
W 19a	R55268	+	+		591486	
W 19B	R55269*	+			591486	
W 37	R55270	+	+	Piallaway	596469	
W127	R55271*	+	+		627468	
W199	R55272	+	+		629445	
W206	R55273*	+	+		631437	
W388	R55274*	+	+ M		633430	
W498	R55275	+	+		635429	

loc.	Catalogue number	Hand specimen	Thin-section	Map sheet and grid reference		Lithology
						Piallaway Trig Ignimbrite Member
W430	R55276	+	+ M	Winton	618494	
Q229	R55277	+	+	Werris Ck.	552299	
Q265a	R55278*	+	+ M	Quipolly	563165	
Q266a	R55279	+	+		567168	
Q279	R55280	+	+		571137	
Q286	R55281	+	+		583149	
Q384	R55282	+	+		586149	
Q391	R55283*	+	+		567159	
Q422	R55285	+	+		671115	
						Piallaway Trig Ignimbrite Member vitrophyres
Q266	R55286	+	+	Quipolly	568168	
Q273	R55287*	+	+		580152	
Q273b	R55288*	+			580152	
Q402	R55289*	+	+		575135	
Q371	R55290	+	+	Werris Ck.	578243	
						Other unnamed ignimbrites Clifton-Carroll Block
W461	R55292	+	+	Winton	511633	(V, Figure 2.2)
W473	R55293	+	+		495569	
W478	R55294	+	+		483547	
W481	R55295	+	+		509533	
W482	R55296	+	+		508531	
						Werrie Syncline
W 14	R55297	+	+	Winton	571492	
W 15	R55298	+	+		574491	
W160	R55299	+	+		621513	
W275b	R55301	+	+	Piallaway	704376	
Q 90	R55302	+	+	Quirindi-B	776012	(W, Figure 2.2) Vitrophyre
						Quirindi Dome
Q338	R55303*	+	+	Werris Ck.	576224	(V, Figure 2.5A) Vitrophyre
Q275	R55304*†	+	+	Quipolly	581149	(Y,Figure 2.2) Vitrophyre 155-4
Q395	R55305	+	+		575151	(Y, Figure 2.2)
Q330	R55306	+	+		586105	Vitrophyre
						Castle Mountain Dome
Q136	R55307	+	+	Quirindi-A	716963	(W, Figure 2.2)
Q136a	R55308	+	+		716963	(W, Figure 2.2) Vitrophyre
Q172	R55309	+	+		706932	(Z, Figure 2.2) Vitrophyre
Q192a	R55310	+	+		716936	(Z,Figure 2.2) Vitrophyre
Q195	R55311	+	+		713934	(Z, Figure 2.2)
Q169	R55312	+	+		731943	
						Kankool area, Figure 5.3
M 5	R55313	+		Quirindi-D	768808	Lava
M 15	R55314	+			811794	Lava
M 27	R55315	+	+		795794	Ignimbrite 2
M 28	R55316	+	+		789803	Ignimbrite 1 (Z,Figure 2.2)
M 37	R55317	+	+		791799	Ignimbrite 1

loc.	Catalogue number	Hand specimen	Thin-section	Map sheet and grid reference		Lithology
						Undifferentiated ignimbrites Kankool
M125	R55318	+	+	Quirindi-D	781787	
M111	R55319	+	+		782778	
M118	R55320	+	+		785779	
M135	R55321	+	+		802756	
M 73	R55322	+	+		788778	
M 54	R55323	+	+		793783	
						Currabubula Formation miscellany
Q324	R55324	+	+	Emblem	763059	Laminated mudstone
Q 47	R55325†	+	+		748156	Granitoid clast 155-1
	R55326	+	+	Winton	560531	Quartzite clast, spiriferid fossils
W 93	R55327	+			590512	Tuffaceous laminated mudstone
W 96	R55328	+			589508	Quartzofeldspathic sandstone
W137a	R55329	+			611524	Conglomerate
W179	R55330	+			564535	Lithic sandstone
W215a	R55331	+		Piallaway	641449	Laminated pebbly mudstone
W513a	R55332	+		Werris Ck.	717328	Rosedale Member, mudstone
W 18	F16381	+		L1841 Winton	591495	Carboniferous plant fossils
W 55b	F16382	+		L1842	622492	
W490	F16383	+		L1843 Piallaway	574423	
W512	F16384	+		L1844	713335	
W513c	F16385	+		L1879 Werris Ck.	717328	*Isopodichnus sp.*
Q274	F16386	+		L1880 Quipolly	582150	*Isopodichnus sp.*
						Temi Formation, Kankool, Figure 5.3
M160b	R55333	+		Quirindi-D		Fossiliferous mudstone
M163	R55334	+	+			'Flint clay' conglomerate (Figure 5.4b)
M168	R55335	+	+			Conglomerate, mafic volcanic clasts (Figure 5.4c)
M160a	R55336	+	+			Fossiliferous 'flint clay' conglomerate (Fig. 5.4d)
						Boggabri Volcanics, Figures 5.5,5.6
K189a	R55338	+		Therribri	025108	Uppermost lava, Fig. 5.6a
K197	R55339	+	+		009099	Upper ignimbrite, top of upper flow unit
K198	R55340	+	+		011096	Upper ignimbrite, base of upper flow unit
K198a	R55341	+	+		011096	
K287	R55342	+			028105	Upper ignimbrite, lower flow unit
K269	R55343	+	+	Boggabri	000079	Upper ignimbrite, lower flow unit
K301	R55344	+	+		016086	Lower ignimbrite
K298	R55345	+	+		007075	Lowest lava, Figure 5.6a

loc.	Catalogue number	Hand specimen	Thin-section	Map sheet and grid reference	Lithology
					Undifferentiated lavas
K209	R55346	+		Therribri 053116	
K215	R55347	+	+	059096	
K255a	R55348	+		044153	
K270a	R55349	+		Boggabri 997027	
K271	R55350	+	+	999044	
K326	R55351	+	+	988080	
K328	R55352	+		093078	
K342	R55353	+	+	985083	
					Undifferentiated ignimbrites
K322	R55354	+	+	Boggabri 977070	*cf.* upper ignimbrite, Figure 5.6a
K337	R55355	+	+	999027	*cf.* upper ignimbrite, Figure 5.6a
K197A	R55356	+		Therribri 009099	Laminated mudstone,
K197	L1839				plant fossils
K323	R55357	+		Boggabri 978069	Accretionary lapilli tuff
					<u>Gunnedah Volcanics</u>
K277	R55359	+		Gunnedah 226745	Ignimbrite Figure 5.6d
					<u>Leard Formation</u>
K223	R55360	+		Therribri 079126	"Flint clay' conglomerate
K229	R55361	+		061129	
					<u>Coombadjha Volcanic Complex</u>
					<u>Pheasant Creek Volcanics</u>
					Crystal-rich ignimbrite
G 1	R55369	+	+ M	Coombadjha 32054235	
G 51	R55370	+	+ M	30504255	
G 60	R55371	+	+ M	33854245	
G 63a	R55372	+	+	33754187	
G 90	R55373	+	+ M	35204185	
G 97	R55374	+	+ M	35404230	
G101	R55375	+	+ M	34254168	
G104a	R55376*	+	+	34154016	
G239	R55377	+	+ M	41354552	
G295	R55378	+	+ M	28604266	
G316	R55379*	+	+	33064068	
G341	R55380	+	+ M	40504708	
G851	R55381	+	+ M	40624640	
G177b	R55382	+	+ M	Washpool 36105181	
G189	R55383	+	+ M	38585207	
G437	R55384*	+	+	28506045	
G473	R55385	+	+ M	33825570	
G489	R55386	+	+ M	31745577	
G543	R55387	+	+ M	27475908	
G581	R55388	+	+ M	Sandy Flat 24626736	
G612	R55389	+	+ M	25306626	

loc.	Catalogue number	Hand specimen	Thin-section	Map sheet and grid reference	Lithology
					<u>Pheasant Creek Volcanics</u>
					Fine grained crystal-poor ignimbrite
G112	R55391	+	+ M	Coombadjha 35954082	
G234	R55392	+	+	39204530	
G315a	R55393	+		33054050	
G339	R55394	+	+ M	40454730	
G405A	R55395	+		Washpool 30405618	
G102	R55397	+		Coombadjha 33924100	Lava breccia
G848	R55398	+		34404025	
G483	R55399	+	+	Washpool 30705882	Microbreccia
G484	R55400	+		30585857	
					Strongly foliated ignimbrite
G113	R55401	+		Coombadjha 35904112	
G182	R55402	+	+ M	Washpool 37005318	
G900	R55403	+		29336112	
					<u>Hianana Volcanics</u>
					Bedded volcaniclastic facies
G84↓	R55405	+	+	Coombadjha 36004560	
G 84a	R55406	+	+	36004560	
G 84b	R55407	+	+	36004560	
G 84↑	R55408	+	+	36004560	
G117↓	R55409	+	+	36004230	
G140b→	R55410	+	+	37824615	
G209a↑	R55411	+	+	37654298	
G223a	R55412	+	+	38024550	
G303	R55413	+	+	37984190	
G177	R55414	+	+	Washpool 36085180	
G515	R55415	+	+	33655478	
G515a	R55416*	+	+	33655478	
G 78c	R55417	+	+	Coombadjha 35004546	Microbreccia
G 82	R55418	+	+	36004606	
G209	R55419	+	+	37654300	Ignimbrite(?)
					Massive porphyry facies
G 78	R55421	+	+ M	Coombadjha 35014544	
G 82	R55422	+	+	36004606	
G116	R55423	+	+	36054220	
G204	R55424	+	+ M	36904456	
G205	R55425*	+	+ M	37104350	
G210a	R55426	+	+	37324275	
G310	R55427	+	+	36784082	
G318a	R55428	+	+ M	35634270	
G719	R55429	+	+ M	39484375	
E 70	R55430	+	+ M	39604295	
					<u>Pi Pi Ignimbrite</u>
G 53	R55432	+	+ M	Coombadjha 30704321	
G 69	R55433	+	+ M	34464318	
G133	R55434*	+		37964930	
G202a	R55435	+	+ M	36904520	
G258a	R55436	+	+ M	29384628	
G294	R55437*	+		28504295	

loc.	Catalogue number	Hand specimen	Thin-section	Map sheet and grid reference		Lithology
						Pi Pi Ignimbrite continued
G304	R55438	+	+ M	Coombadjha	37954282	
G338	R55439	+	+ M		40274752	
G359	R55440	+	+ M		37754276	
G330	R55441	+	+ M	Washpool	36625146	
G335	R55442	+	+ M		37955030	
G421a	R55443	+	+ M		28935648	
G468	R55444*	+			34705365	
G621	R55445	+	+ M	Sandy Flat	24006877	
G290c	R55446	+	+	Coombadjha	29004675	(contact with Dundee Rhyodacite)
						Babepercy Volcanics
						Volcaniclastic rocks
E 1	R55447	+	+		30944506	
G24b↑	R55448	+	+		31014496	
G 25	R55449	+	+		30704510	
E 64	R55450	+			30704510	
G 24	R55451	+			31014496	
						Dundee Rhyodacite
						Normal facies ignimbrite
G 72	R55453	+	+ M	Coombadjha	34704386	
G 77	R55454	+	+ M		35064490	
G112a	R55455	+	+		35984080	
G135	R55456*	+			37684830	
E 46	R55457	+	+ M		31704877	
G413	R55458	+	+	Washpool	27865450	
G413a	R55459	+	+ M		27865450	
G414	R55460	+	+		27925484	
G415	R55461	+	+		28245545	
G417	R55462	+	+		28645580	
G463	R55463	+	+		28876367	
G464	R55464	+	+ M		28506378	
G530	R55465*	+	+ M	Coombadjha	39454915	
G532	R55466	+	+ M	Washpool	28305746	
G981	R55467	+	+		31656245	
G700	R55468	+	+ M	Sandy Flat	22947720	
G703	R55469	+	+ M		24267706	
						Near-base, Normal facies ignimbrite
G 11b	R55471	+	+	Coombadjha	33254506	
G 12	R55472	+	+ M		33374532	
G120a	R55473	+	+ M		35954308	
G228	R55474	+	+ M		37604492	
G258	R55475	+	+ M		29434630	
G290	R55476	+	+		29004675	
G290b	R55477	+	+ M		29004675	
G715	R55478*	+	+		38704436	
G716	R55479	+	+ M		38804425	
G853	R55480*	+	+ M		40074653	
G863	R55481*	+	+ M		27884401	
G932a	R55482	+	+		39104268	

loc.	Catalogue number	Hand specimen	Thin-section	Map sheet and grid reference		Lithology
						Near-base Normal facies continued
G166a	R55483	+	+	Washpool	35055060	
G397	R55484	+	+		29925360	
G398	R55485	+			30365370	
G402	R55486	+	+		30755585	
G425a	R55487	+	+ M		28905722	
G492	R55488	+	+ M		31755503	
G523	R55489	+	+ M		34555326	
G544a	R55490	+	+		27385900	
G897a	R55491	+	+		30556215	
G1005	R55492	+	+		28125840	
G447	R55493	+	+	Spirabo	26735972	
						Basal facies-ignimbrite
G426	R55496	+	+	Washpool	28805750	
G438	R55497	+	+ M		28386116	
G439	R55498	+	+		27886149	
G534	R55499	+	+		28605775	
G825a	R55500	+	+		28905875	
G826	R55501	+	+ M		28775855	
G827a	R55502	+	+		28205845	
G838	R55503	+	+		29955655	
G973a	R55504	+	+		29466261	
						Basal facies-porphyritic dacite
G 37	R55506	+	+ M	Coombadjha	31754521	
G 80a	R55507	+	+		35024635	
G 87	R55508	+	+		35204330	
G141	R55509	+	+ M		36924613	
G235a	R55510*	+	+		39404530	
G237	R55511	+	+		39804520	
G237A	R55512	+	+		39804520	
G249	R55513	+	+		40314685	
G168a	R55514	+	+ M	Washpool	34465065	
G333	R55515*	+	+ M		35955094	
G420	R55516	+	+		28855632	
G421	R55517	+	+		28935647	
G440	R55518	+	+		27856110	
G535[1]	R55519	+	+		28775830	
G554	R55520*	+			28456142	
G897	R55521	+	+		30556214	(sheared)
						Basal facies-bedded tuff
G153a	R55523	+	+	Coombadjha	35204838	
G235	R55524	+	+		39404530	
G236	R55525	+	+		35524525	
G290a	R55526	+	+		29004675	
G120	R55527	+	+		35964308	
G441	R55528	+	+	Washpool	27506071	
G827b	R55529	+	+		28165842	
G1005b	R55530	+	+		28105840	
G 80	R55533	+	+	Coombadjha	35024634	Basal facies - "breccia"
G 80a	R55534	+	+		35044640	
G 80b	R55535	+	+		35044640	
G153	R55536	+	+		35204838	

loc.	Catalogue number	Hand specimen	Thin-section	Map sheet and grid reference	Lithology
					Basal facies-"breccia" continued
G231a	R55537	+	+	Coombadjha 38804509	
G166	R55538	+		Washpool 35065058	
G169	R55539	+	+	34385060	
G169	R55540	+	+	34385060	
G409	R55541	+	+	29015565	
G420A	R55542	+	+	28855632	
G420B	R55543	+	+	28855632	
G533	R55544	+	+	28545770	
G827	R55545	+	+	28205843	
G839	R55546	+	+	29555622	
G839A	R55547	+	+	29555622	
G1005a	R55548	+	+	28105840	
					Moonta Gully Adamellite
G238A	R55552	+	+	Coombadjha 40104525	
G238B	R55553	+	+	40104525	
G309	R55554	+	+ M	36604095	
G313	R55555	+		33153962	
G342	R55556	+	+ M	40704780	
G843	R55557*	+		33553885	
G850	R55558	+	+	40754635	
G188	R55559*	+		Washpool 38405526	
G478	R55560	+	+	32705920	
G501	R55561	+	+	35205586	
G971	R55562	+	+ M	29276213	
					OBX Creek Intrusion
G406	R55564	+	+	Washpool 29925586	
G407a	R55565	+	+	29685578	
G404	R55566	+		30555601	
					Weat Gully Porphyry
G506	R55567	+	+	Washpool 33975155	
G507A	R55568	+	+	34225135	
G503	R55569	+	+	33545215	
					Intrusions similar to the Moonta Gully Adamellite
G455	R55570	+		Malara Ck. 28906545	
G457	R55571	+		30456422	
G465	R55572	+		Washpool 28406400	
G559	R55573	+	+	27836365	
G893	R55574	+	+	31806170	
G778	R55575	+	+	Tenterfield 24068806	
G782	R55576	+	+	24068910	
G807A	R55577	+	+	24059005	
					Other intrusions
G448	R55578	+	+	Spirabo 26605890	
G448a	R55579	+	+	26605890	
G841A	R55581	+	+	26465995	
G842	R55582	+	+	26406015	
G365	R55583	+		Coombadjha 29604100	
G713	R55610*	+	+ M	Sandy Flat 09007765	Dundee Rhyodacite - Brassington

loc.	Catalogue number	Hand specimen	Thin-section	Map sheet and grid reference		Lithology
G810	R55611	+	+ M	Tenterfield	11288535	Dundee Rhyodacite - Tenterfield
G811	R55612*	+	+		11098456	
G812	R55613*	+	+ M		10648311	
G575	R55614	+	+		14258122	
G868	R55615	+	+ M	Stanthorpe	90809431	Dundee Rhyodacite - Tarban
G869	R55616*	+	+ M		94209415	
A 10	R55617	+	+ M	Clive	67253915	Dundee Rhyodacite - Dundee